

Willow tree algorithms for pricing Guaranteed Minimum Withdrawal Benefits under jump-diffusion and CEV models

Bing Dong¹, Wei Xu^{2†} and Yue Kuen Kwok³

^{1,2} School of Mathematical Sciences, Tongji University,
Shanghai, China, 200092

³ Department of Mathematics, Hong Kong University of Science and Technology,
Hong Kong, China

Abstract

This paper presents the willow tree algorithms for pricing variable annuities with Guaranteed Minimum Withdrawal Benefits (GMWB), where the underlying fund dynamics evolves under the Merton jump-diffusion process or constant-elasticity-of-variance (CEV) process. The GMWB rider gives the policyholder the right to make periodic withdrawals from his policy account throughout the life of the contract. The dynamic nature of the withdrawal policy allows the policyholder to decide how much to withdraw on each withdrawal date, or even surrender the contract. For numerical valuation of the GMWB rider, we use the willow tree algorithms that adopt more effective placement of the lattice nodes based on better fitting of the underlying fund price distribution. When compared with other numerical algorithms, like the finite difference method and fast Fourier transform method, the willow tree algorithms compute GMWB prices with significantly less computational time to achieve similar level of numerical accuracy. The design of our pricing algorithms also includes an efficient search method for the optimal dynamic withdrawal policies. We perform sensitivity analysis of various model parameters on the prices and fair participating fees of the GMWB riders. We also examine effectiveness of delta hedging when the fund dynamics exhibits various levels of jump.

1 Introduction

Variable annuities are annuity products with equity participation that are sold by insurance companies. The policyholder pay an upfront premium and the proceeds are invested in his individual

The works of Bing Dong and Wei Xu were partially supported by the Natural Science Foundation of China (Project Number: 71771175, U1811462) and the Fundamental Research Funds for the Central Universities. The work of Yue Kuen Kwok was supported by the General Research Fund (Project Number: 16302416) of the Hong Kong Research Grants Council.

[†]Corresponding author. E-mails: ¹ dong.bing@tongji.edu.cn; ² wdxu@tongji.edu.cn; ³ maykwok@ust.hk.

wealth account that is made up of mutual funds and other investment instruments. Since late 1990s, insurance companies started to add various forms of guarantee riders into variable annuity products. Since then, we have witnessed significant growth in the variable annuities markets. The variable annuity net assets in the world amount to 1.95 trillion US dollars at the end of the first quarter of 2018 (Source: Morningstar, Inc. and Insured Retirement Institute).

One of the most popular guarantee riders in variable annuity products is the Guaranteed Minimum Withdrawal Benefits (GMWB). The GMWB allows the policyholder to withdraw a fixed percentage of the total annuity premium each year regardless of the market performance of the asset portfolio. The withdrawal payments are guaranteed until the total premium is recovered, even when the policyholder's personal wealth account has depleted to zero value due to poor performance of the asset portfolio. On the other hand, under favorable returns of investment such that the wealth account stays positive at maturity, the policyholder is entitled to receive at maturity the remaining balance in either the wealth account or guarantee account, whichever is higher. Under the dynamic guarantee clause of the GMWB, the policyholder is allowed to withdraw any amount within the limit of the wealth account, which can be either below, at or above the contractual amount. In addition, the policyholder has the right to surrender the contract prematurely, which is equivalent to complete withdrawal of the whole wealth account. The contract usually imposes certain provisions to discourage withdrawal above the contractual amount. Typically, a penalty charge is applied on the withdrawal amount that is above the contractual amount. Another disincentive measure to discourage excess withdrawal is the imposition of the reset provision, where the guarantee account may be reset to the minimum of the prevailing guarantee account level and wealth account value. The insurer charges a proportional participating fee per annum on the wealth account in order to fund the GMWB rider. When selling the GMWB products, insurance companies are concerned not to charge the participating fees too low that are not sufficient to cover the hedging costs of the embedded guarantees.

Under the simplified assumption that the withdrawal policy is static, which means the policyholder always withdraws the contractual amount on each withdrawal date and never surrenders, Milevsky and Salisbury (2006) show that the value function of the GMWB product can be decomposed into a quanto Asian put option and a generic term certain annuity. Under the optimal dynamic withdrawal policy, the policyholder optimally determines the withdrawal amount on each withdrawal date so as to maximize the value function of the GMWB rider. This benchmark case of value maximization results in the highest cost of hedging borne by the insurer (Moenig and Bauer,

2011). In reality, the policyholder may adopt some suboptimal withdrawal policies; for example, withdrawal and surrender decisions are made based on the moneyness of the value of the guarantee. Under the continuous time model of optimal dynamic withdrawal, the continuous withdrawal rate becomes a stochastic control variable. Dai *et al.* (2008) derive the Hamilton-Jacobi-Bellman variational inequalities formulation of the resulting singular stochastic control model. They also propose the finite difference scheme coupled with the penalty approximation method to price GMWB products under both continuous withdrawal rate and discrete withdrawals. Huang and Forsyth (2012) present the rigorous convergence proof of the penalty approximation schemes for solving the GMWB pricing models. Other versions of the singular stochastic control models and construction of various finite difference methods and lattice tree schemes can be found in Milevsky and Salisbury (2006), Bauer *et al.* (2008), Huang *et al.* (2012), Yang and Dai (2013), and Forsyth and Vetzal (2014). Under the continuous withdrawal model, Huang and Kwok (2014) perform full mathematical characterization of the optimal withdrawal policies. Their bang-bang results for the optimal withdrawal strategies fall into three choices: zero withdrawal, withdrawal at the contractual rate and complete surrender. However, Azimzadeh and Forsyth (2015) show that the above bang-bang optimal withdrawal policies for the GMWB pricing model become invalid under discrete withdrawals. Without the simplification offered by the bang-bang withdrawal strategies, the design of an effective search algorithm for the optimal withdrawal amounts under discrete withdrawals remains a challenge.

Most earlier research papers on pricing GMWB assume the geometric Brownian motion for the underlying fund dynamics, constant interest rate and volatility. The recent works show various extensions on the choice of fund dynamics, design of numerical schemes and implementation of hedging strategies. Chen *et al.* (2008) include jump in the fund price dynamics and explore whether typical participating fees charged on GMWB contracts are sufficient to cover the cost of hedging the embedded guarantees. They explore the effects of various modeling assumptions on the optimal withdrawal strategy of the policyholder and their effects on the guarantee value associated with sub-optimal withdrawal behaviors. Peng *et al.* (2012) derive analytic approximation of the lower and upper bounds for the price of GMWB under the Vasicek interest rate and static withdrawals. For numerical pricing under the Vasicek interest rate and dynamic withdrawals, Shevchenko and Luo (2017) develop the two-dimensional Gauss-Hermite quadrature scheme to perform expectation calculations of the value function over consecutive withdrawal dates. Kang and Ziveyi (2018) use the Method of Lines algorithm to analyze the policyholder surrender behavior under stochastic interest rate and volatility. Gudkov *et al.* (2018) use the componentwise splitting approach in the

multidimensional finite difference scheme to price GMWB products under stochastic interest rate, volatility and mortality. Other numerical schemes for pricing GMWB products include the flexible lattice tree method (Costabile, 2017) and fast Fourier transform method (Ignatieva *et al.*, 2016). With known analytic forms of the characteristic functions of the various choices of the Lévy processes for the underlying fund dynamics, Bacinello *et al.* (2016) use the Fourier space time-stepping method to price GMWB products under different Lévy processes and policyholder behaviors. Alonso-Garcia *et al.* (2018) design more refined recursive dynamic programming procedure coupled with the Fourier cosine transform method for pricing and hedging GMWB products. They develop a local risk minimization approach to hedge inter-withdrawal date risks and consider various choices of risk measures under the general Lévy framework.

Though the academic literature reveals a wide range of numerical schemes that have been developed for pricing GMWB products under a variety of fund dynamics, there remains the quest for more efficient numerical scheme to perform the expectation calculations of the value function in the backward induction procedure and effective search for the optimal withdrawal policies. The finite difference and lattice tree methods normally require a large number of time steps to perform expectation calculations between consecutive withdrawal dates. On the other hand, the Fourier transform method and numerical quadrature scheme can perform numerical integration between consecutive withdrawal dates in one time step. However, in the fast Fourier transform method, one has to perform transformation of the value function from the Fourier domain to the real domain on each withdrawal date in order to implement the jump conditions on the wealth account and guarantee account to model the associated withdrawal or surrender event. For the one-step Gauss-Hermite quadrature scheme, it requires known analytic formula of the transition density function of the fund dynamics between consecutive withdrawal dates. Besides, it is also desirable to develop more efficient search algorithm for optimal withdrawal strategies that goes beyond the direct iteration search used in most existing published works.

In this paper, we propose the willow tree algorithm for performing effective expectation calculations of the value function between consecutive withdrawal dates in the GMWB pricing model and an efficient constrained optimization algorithm that searches for optimal dynamic withdrawals. The willow tree method was first proposed by Curran (2001), and the method is later applied by various researchers to price various path dependent options and exotic derivatives (Xu *et al.*, 2013; Xu and Yin, 2014; Lu *et al.*, 2017; Lu and Xu, 2017; Wang and Xu, 2018). Improved computational efficiency is achieved in the willow tree algorithm via the more efficient construction of the willow

tree nodes that better simulate the underlying fund dynamics when compared with the usual lattice tree algorithms and Markov chain method. The knowledge of the probability distribution of the underlying fund dynamics is used in the construction of the willow tree. Unlike the finite difference algorithm where uniform spacing of layers of nodes is adopted, we use the first four order moments of the fund dynamics to determine the layers of nodes in the willow tree. In Section 3, we show how to construct the willow tree for the following two fund value processes: Merton's jump-diffusion process (Merton, 1976) and constant elasticity of variance (CEV) process (Cox, 1975). In fact, the willow tree method can be extended to Kou's jump-diffusion model, general Lévy processes and stochastic volatility processes. For these complex stochastic fund value processes, assuming availability of the corresponding analytic moment generating function, one can employ the fast Fourier transform algorithm to compute the higher order moments and construct the willow tree accordingly. Details of the procedure can be found in Yao *et al.* (2019). Once the corresponding willow tree structure has been formulated, the GMWB pricing scheme proposed in this paper can be applicable to a wide variety of fund value processes with jumps, not just limited to Merton's jump-diffusion process and CEV process. Unlike the finite difference schemes, the inclusion of jump dynamics in the fund value process does not increase an extra dimension of the computation procedure in the willow tree algorithms. Our GMWB pricing algorithm also includes an efficient search procedure for the optimal withdrawal strategies, which can be formulated as an one-dimensional constrained optimization problem.

The remaining sections of this paper are organized as follows. In the next section, we present the pricing model formulation of the GMWB. The jump conditions on the wealth account and guarantee account across a withdrawal date that model various reset provisions and surrender events are discussed. In Section 3, we present the construction of the willow tree algorithm under Merton's jump-diffusion process and CEV process, together with the constrained optimization algorithms for searching optimal withdrawals. In Section 4, we show comparison of performance of our willow tree algorithm with other numerical methods and discuss the impact of penalty charges on the optimal withdrawal policies. We perform sensitivity analysis of various model parameters on the prices and fair participating fees of the GMWB riders. Also, we examine effectiveness of delta hedging under jump dynamics of the fund value process. Conclusive remarks are presented in the last section.

2 Model formulation

We consider a variable annuity with the GMWB rider expiring in T years. At the inception of the contract, the initial upfront payment W^0 paid by the policyholder is invested into an asset fund chosen by the policyholder. With withdrawals spread over the life of the variable annuity contract, the GMWB rider guarantees to return the entire initial upfront payment irrespective of the market performance of the asset fund underlying the policyholder's wealth account. Besides the wealth account of the policyholder's personal portfolio, the guarantee account also keeps track of the remaining guaranteed amount to be received by the policyholder in the remaining life of the GMWB contract. At initiation, the guaranteed withdrawal account is W^0 since there has not been any withdrawal. Let $W(t)$ and $A(t)$ denote the respective value process of the wealth account and guaranteed withdrawal account, $0 \leq t \leq T$. Note that $W(0) = A(0) = W^0$. Let G denote the contractual withdrawal amount on each withdrawal date. Suppose we assume annual withdrawals, then G is set to be W^0/T . The withdrawal amount is allowed to be larger than G , but the policyholder has to pay a penalty for the amount that exceeds G . On the other hand, the insurer charges the policyholder an annual participating fee α based on the value of the wealth account. Suppose withdrawals are allowed on N preset dates during the contractual period $[0, T]$, where the uniformly distributed withdrawal dates are $t_n = n\Delta t$, $n = 1, 2, \dots, N$, $\Delta t = \frac{T}{N}$. We assume that surrender of the contract can only occur on a withdrawal date.

We consider two stochastic processes for the asset fund value process $S(t)$, whose dynamics under a risk neutral measure Q are governed by

(1) Jump-diffusion model (Merton, 1976)

$$\frac{dS(t)}{S(t)} = (r - \lambda\bar{k})dt + \sigma dB(t) + [Y(t) - 1] dN(t), \quad (2.1)$$

where r is the constant risk free interest rate, $B(t)$ is the standard Q -Brownian motion, $\bar{k} = E[Y(t) - 1]$, $\ln Y(t) \sim N(\alpha_J, \sigma_J^2)$, and $N(t)$ follows the Poisson process with constant intensity λ . Here, $N(\mu, \sigma^2)$ represents the normal distribution with mean μ and variance σ^2 . The Merton jump-diffusion process reduces to the usual geometric Brownian motion when the jump component vanishes.

(2) CEV model (Cox, 1975)

$$dS(t) = rS(t)dt + \sigma S(t)^\beta dB(t), \quad (2.2)$$

where r is the risk free interest rate, $B(t)$ is the standard Q -Brownian motion, σ is a constant and β is the constant elasticity of variance parameter. The parameter β controls the leverage between

volatility and asset fund value. When $0 < \beta \leq 1$ (commonly observed in equity markets), we observe the so-called leverage effect, where volatility is negatively related to fund value level. Conversely, when $\beta > 1$, which is often observed in commodity markets (German and Shih, 2009), volatility tends to increase as price increases (so-called negative leverage effect). In this paper, we assume $0 < \beta \leq 1$, though our pricing algorithm is also applicable for $\beta > 1$. The CEV model degenerates into the geometric Brownian motion model when $\beta = 1$.

Under the GMWB rider, even when W_t hits zero before maturity of the contract, annual withdrawals would continue until the entire guaranteed withdrawal account is depleted. Let $W(t_n^-)$ and $W(t_n^+)$ denote the wealth account value right before and after the withdrawal date t_n , respectively, and apply the same notational interpretation for $A(t_n^-)$ and $A(t_n^+)$. Let ξ_n be the withdrawal amount at t_n . The wealth account value has a downward jump of ξ_n right after withdrawal while the asset fund value process $S(t)$ remains continuous across a withdrawal date. Under the static withdrawal clause, ξ_n is set to be G . On the other hand, the dynamic withdrawal clause allows ξ_n to take any value between 0 and $A(t_n^-)$. Also, the policyholder may surrender the contract at t_n , corresponding to taking $\xi_n = W(t_n^-)$. The time evolution of the wealth account value $W(t)$ and guaranteed withdrawal account $A(t)$ on the path of the fund value $S(t)$ and the downward jump on $W(t)$ and $A(t)$ across the withdrawal date t_n are described as follows.

- At time t_n^- , the wealth account value $W(t_n^-)$ is given by

$$W(t_n^-) = W(t_{n-1}^+) \frac{S(t_n)}{S(t_{n-1})} e^{-\alpha \Delta t}, \quad (2.3a)$$

where α is the annualized participating fee continuously charged by the insurer. Since there is no withdrawal during (t_{n-1}, t_n) , the guaranteed withdrawal account value remains the same, so we have

$$A(t_n^-) = A(t_{n-1}^+). \quad (2.3b)$$

- Note that ξ_n may be larger than $W(t_n^-)$ due to the guarantee rider and the wealth account has the zero floor value. At time t_n^+ , right after withdrawal of amount ξ_n , the wealth account value becomes

$$W(t_n^+) = \max\{W(t_n^-) - \xi_n, 0\}. \quad (2.4)$$

- If there is no reset provision, then the guaranteed withdrawal account $A(t_n^+)$ is given by

$$A(t_n^+) = \max\{A(t_n^-) - \xi_n, 0\}. \quad (2.5a)$$

The downward jump on $A(t)$ across t_n is complicated by the reset provision, which is imposed to discourage excess withdrawal beyond the contractual amount. In this paper, we use the ‘pro-rata adjustment’ reset provision as proposed in Bacinello *et al.* (2016), where $A(t_n^+)$ is given by

$$A(t_n^+) = \begin{cases} A(t_n^-) - \xi_n, & \xi_n \leq \min\{G, A(t_n^-)\}, \\ \max \left\{ \min \left\{ A(t_n^-) - \xi_n, A(t_n^-) \frac{W(t_n^-) - \xi_n}{W(t_n^-)} \right\}, 0 \right\}, & \xi_n > \min\{G, A(t_n^-)\}. \end{cases} \quad (2.5b)$$

Under excessive withdrawal beyond $\min\{G, A(t_n^-)\}$, the guaranteed withdrawal account is penalized by setting $A(t_n^+)$ to be the minimum of $A(t_n^-) - \xi_n$ and $A(t_n^-)$ multiplied by the pro-rata factor $\frac{W(t_n^-) - \xi_n}{W(t_n^-)}$.

There are some other reset provisions, like the one adopted in Alonso-García *et al.* (2018), where $A(t_n^+)$ is given by

$$A(t_n^+) = \begin{cases} \max\{A(t_n^-) - \xi_n, 0\}, & \xi_n \leq G, \\ \max \{ \min \{ A(t_n^-) - \xi_n, W(t_n^-) - \xi_n \}, 0 \}, & \xi_n > G. \end{cases} \quad (2.5c)$$

This reset provision discourages excess withdrawal beyond G when $W(t_n^-) < A(t_n^-)$.

There is a penalty charge at the rate η on the excess amount of withdrawal above G . The cash amount received by the policyholder on the withdrawal date t_n is given by

$$C(t_n) = \begin{cases} \xi_n & \text{if } 0 \leq \xi_n \leq G \\ G + (1 - \eta)(\xi_n - G) & \text{if } \xi_n > G \end{cases}. \quad (2.6)$$

On maturity date T , the policyholder receives either the remaining balance in the wealth account $W(t_N^-)$ or cash amount $C(t_N)$, whichever is higher.

The value function $V(W(t_n^-), A(t_n^-), t_n^-)$ of the GMWB contract at time t_n^- is given by the sum of discounted cash amounts received by the policyholder on all future withdrawal dates $t_n, t_{n+1}, \dots, t_{N-1}$, and at maturity T , subject to the optimal choices of the withdrawals $\xi = (\xi_n, \xi_{n+1}, \dots, \xi_{N-1})$. Assuming that the policyholder survives beyond T and no surrender occurs during the life of the contract, we have

$$\begin{aligned} & V(W(t_n^-), A(t_n^-), t_n^-) \\ &= \sup_{\xi} \left\{ E_Q \left[e^{-r(T-t_n)} \max \{ W(t_N^-), C(t_N) \} + \sum_{j=n}^{N-1} e^{-r(t_j-t_n)} C(t_j) \mid W(t_n^-), A(t_n^-) \right] \right\}. \end{aligned} \quad (2.7)$$

The other two risk factors affecting the value of GMWB are the mortality risk and early surrender. Suppose the policyholder dies within $(t_{n-1}, t_n]$, the contract is terminated and the wealth account value $W(t_n^-)$ is returned to the beneficiary at t_n . Under the mix withdrawals with surrender provision, the policyholder has the option to withdraw the full wealth account value and terminate the contract on a withdrawal date. We consider the modification of the model formulation under inclusion of mortality risk and surrender provision in Section 3.2.

3 Construction of the willow tree and search algorithm of optimal withdrawals

We consider the log-return of the fund unit $S(t)$, where $X(t) = \ln S(t)$ and construct the willow tree with respect to the underlying dynamics of $X(t)$. On each withdrawal date t_n , $n = 1, 2, \dots, N$, we sample m possible log-returns X_i^n , $i = 1, 2, \dots, m$, from the distribution of the process $X(t)$ at t_n . The probability of transition from node X_i^n to node X_j^{n+1} on the next withdrawal date t_{n+1} is characterized by the transition probability p_{ij}^n . In Figure 1, the willow tree structure is constructed with 4 withdrawal dates and 5 possible $X(t)$ values on each withdrawal date. At initial time $t_0 = 0$, taking $S(0) = 1$, there is only one node at t_0 with $X(0) = 0$. On each withdrawal date, the nodes are chosen to fit the corresponding distribution of the underlying fund dynamics. The transition probabilities are determined to approximate the stochastic evolution of the fund dynamics between consecutive withdrawal dates. Provided that we put enough number of nodes on each withdrawal date, it is not necessary to assign intermediate time steps between consecutive withdrawal dates in the willow tree lattice. Since withdrawals and updating of $W(t)$ and $A(t)$ occur only on withdrawal dates, it is superfluous to compute the value function at intermediate times between consecutive withdrawal dates as in the usual lattice tree algorithms and finite difference methods. The total number of nodes in the willow tree lattice would be the number of space nodes on each withdrawal date (typically 50 to 100) multiplied by the number of withdrawal dates.

3.1 Construction of the willow tree under Merton's jump-diffusion process

We discuss the construction of the willow tree under Merton's jump-diffusion process and calculation of the transition probability p_{ij}^n from node X_i^n to node X_j^{n+1} . The mean, variance, skewness and kurtosis of the increment over Δt time interval of Merton's jump-diffusion process as governed by

eq. (2.1) are found to be (Ballotta and Kyriakou, 2015):

$$\begin{aligned}
\text{Mean} &= [r - \frac{\sigma^2}{2} - \lambda(e^{\alpha_J + \sigma_J^2/2} - 1) + \lambda\alpha_J]\Delta t \\
\text{Variance} &= (\sigma^2 + \lambda\alpha_J^2 + \lambda\sigma_J^2)\Delta t \\
\text{Skewness} &= \frac{\lambda(\alpha_J^3 + 3\alpha_J\sigma_J^2)}{\sqrt{\Delta t}(\sigma^2 + \lambda\alpha_J^2 + \lambda\sigma_J^2)^{3/2}} \\
\text{Kurtosis} &= \frac{\lambda(\alpha_J^4 + 6\alpha_J^2\sigma_J^2 + 3\sigma_J^4)}{\Delta t(\sigma^2 + \lambda\alpha_J^2 + \lambda\sigma_J^2)^2}.
\end{aligned} \tag{3.1}$$

The Johnson curve transformation (Johnson, 1949) transforms a standard normal variable into an arbitrary random variable via matching the first four moments. The nodes are set to be

$$X_i^n = \varepsilon g^{-1}\left(\frac{z_i - \gamma}{\delta}\right) + \nu, \tag{3.2}$$

where the parameters γ, δ, ν and ε can be determined by the algorithm proposed in Hill and Holder (1976), z_i are the discrete values of the standard normal distribution and the function $g^{-1}(u)$ is defined by

$$g^{-1}(u) = \begin{cases} e^u & \text{for the lognormal family,} \\ \frac{e^u - e^{-u}}{2} & \text{for the unbounded family,} \\ \frac{1}{1+e^{-u}} & \text{for the bounded family,} \\ u & \text{for the normal family.} \end{cases} \tag{3.3}$$

The m possible log-returns X_i^n , $i = 1, 2, \dots, m$, are selected to match the first four moments of $X(t_n)$ by the Johnson curve transformation. The key consideration in sampling X_i^n is to select $\{z_i\}$ from the standard normal distribution. According to Xu *et al.* (2013), a sequence of $\{(z_i, q_i)\}$, $i = 1, 2, \dots, m$, is generated to approximate the standard normal distribution, where z_i is some discrete value of the standard normal distribution and q_i is the corresponding probability of z_i . The generation of the sequence starts from a sequence of $\{\tilde{q}_j\}$, where

$$\tilde{q}_j = (j - 0.5)^\vartheta/m, \quad \text{and} \quad \tilde{q}_{m+1-j} = \tilde{q}_j, \quad \text{for } j = 1, 2, \dots, m/2, \quad \text{and } 0 \leq \vartheta \leq 1.$$

The parameter ϑ controls the distance between \tilde{q}_i . When $\vartheta = 0$, all \tilde{q}_i are identical. When $\vartheta > 0$, the probabilities close to the tail of the standard normal distribution are small while those near the center of the standard normal distribution are large. Similar to Xu *et al.* (2013), we take $\vartheta = 0.6$ in our calculations. The sequence $\{q_i\}$ is then normalized by

$$q_i = \tilde{q}_i / \sum_{j=1}^m \tilde{q}_j \quad \text{for } i = 1, 2, \dots, m.$$

Next, we determine the sequence of $\{z_i\}$ by the solution of the following nonlinear least squares problem:

$$\min_{z_i} \left(\sum_{i=1}^m q_i z_i^4 - 3 \right)^2$$

such that $\sum_{i=1}^m q_i z_i = 0$, $\sum_{i=1}^m q_i z_i^2 = 1$, and $Z_{i-1} \leq z_i \leq Z_i$. Here, $Z_i = N^{-1}(\sum_{j=1}^i q_j)$, $i = 1, 2, \dots, m-1$, $Z_0 = -\infty$ and $Z_m = \infty$ so that the pair $\{(z_i, q_i)\}$ satisfy the properties of the standard normal distribution, with mean equals zero, variance equals one and kurtosis equals three. In summary, using the discrete sampling z_i in the standard normal distribution, we can map z_i to X_i^n by the Johnson curve transformation via matching the first four moments of $X(t_n)$.

On the other hand, the transition probability p_{ij}^n from X_i^n to X_j^{n+1} can be estimated by (Xu and Yin, 2014)

$$p_{ij}^n = P(A < X_j^{n+1} < B | X_i^n) = \int_A^B \sum_{l=0}^{\infty} \frac{e^{-\lambda \Delta t} (\lambda \Delta t)^l}{l!} \frac{1}{\sqrt{2\pi} \sigma_l} \exp \left[-\frac{(x - \mu_l)^2}{2\sigma_l^2} \right] dx, \quad (3.4)$$

where $A = (X_{j-1}^{n+1} + X_j^{n+1})/2$, $B = (X_{j+1}^{n+1} + X_j^{n+1})/2$, $\mu_l = X_i^n + (r - \lambda \bar{k} - \frac{\sigma^2}{2})\Delta t + l\alpha_J$ and $\sigma_l^2 = \sigma^2 \Delta t + l\sigma_J^2$.

The two-step procedure of constructing the willow tree nodes involves the determination of the willow tree nodes and transition probabilities. These two steps can be performed in a similar manner for other underlying fund dynamics. The extension of the above two-step procedure to the CEV process is presented in Appendix A. Once the willow tree structure has been constructed, the same GWMB pricing procedure can be applied to all stochastic fund value processes based on the willow tree structure.

3.2 Numerical valuation framework with discrete withdrawals

First we determine the maximum wealth account value $W(t)$ at t_n^- . Taking $S_0 = 1$ for simplicity, suppose $S(t_n^-)$ reaches S_i^n at t_n^- , we have

$$W_{i,\max}^n = W^0 S_i^n e^{-\alpha n \Delta t}. \quad (3.5)$$

In the willow tree lattice, we consider K discrete values of W_i^n in the interval $[0, W_{i,\max}^n]$, where

$$W_{i,k}^n = \frac{k-1}{K-1} W_{i,\max}^n, \quad k = 1, 2, \dots, K. \quad (3.6)$$

Denote $V_{i,k}^n \equiv V(S_i^n, W_{i,k}^n, t_n)$ as the numerical approximation value of the GMWB. The calculation of the GMWB value $V_{i,k}^n$ is based on the following backward induction of the willow tree for the fund value process $\{S_i^n\}$.

- At maturity $t_N = T$, for each mutual fund price S_i^N , the K possible wealth account values $W_{i,k}^N$ are determined by (3.6). The corresponding GMWB value $V_{i,k}^N$ at T is calculated by

$$V_{i,k}^N = \max \{W_{i,k}^N, G\}, \quad \text{for } i = 1, 2, \dots, m, \quad k = 1, 2, \dots, K. \quad (3.7)$$

- At time $t_{N-1} = (N-1)\Delta t$, for each mutual fund price S_i^{N-1} , there are K possible account values $W_{i,k}^{N-1}$. Given the withdrawal amount ξ_{N-1} and assuming that the fund price evolves from S_i^{N-1} to S_j^N with wealth account value $W_{i,k}^{N-1}$, the corresponding wealth account value at t_N^- becomes

$$\bar{W}_j^N = \max \left\{ W_{i,k}^{N-1} - \xi_{N-1}, 0 \right\} \frac{S_j^N}{S_i^{N-1}} e^{-\alpha \Delta t}. \quad (3.8)$$

Since \bar{W}_j^N must fall into $[0, W_{j,\max}^N]$, so there exists an integer k^* such that $W_{j,k^*}^N \leq \bar{W}_j^N \leq W_{j,k^*+1}^N$. The corresponding GMWB value with account value \bar{W}_j^N can be estimated by a linear interpolation of V_{j,k^*}^N and V_{j,k^*+1}^N . We have

$$\bar{V}_j^N = \lambda_j^N V_{j,k^*+1}^N + (1 - \lambda_j^N) V_{j,k^*}^N, \quad (3.9)$$

where

$$\lambda_j^N = \frac{\bar{W}_j^N - W_{j,k^*}^N}{W_{j,k^*+1}^N - W_{j,k^*}^N}.$$

After considering all possible scenarios of the fund price evolution from S_i^{N-1} to S_j^N , $j = 1, 2, \dots, m$, and under the wealth account value $W_{i,k}^{N-1}$, the corresponding GMWB value $V_{i,k}^{N-1}$ can be estimated as

$$V_{i,k}^{N-1} = e^{-r\Delta t} \sum_{j=1}^m p_{ij}^{N-1} \bar{V}_j^N + \varphi(\xi_{N-1}), \quad i = 1, \dots, m, \quad \text{and } k = 1, \dots, K, \quad (3.10)$$

where p_{ij}^{N-1} is the transition probability from S_i^{N-1} to S_j^N , and $\varphi(\xi_{N-1})$ is the net cash amount received by the policyholder with respect to the withdrawal amount ξ_{N-1} . This gives

$$\varphi(\xi_{N-1}) = \begin{cases} \xi_{N-1}, & \xi_{N-1} \leq G, \\ G + (1 - \eta) \left(\min\{\xi_{N-1}, L_{i,k}^{N-1}\} - G \right), & \xi_{N-1} > G, \end{cases} \quad (3.11)$$

where η is the penalty charge on the portion exceeding the contractual withdrawal amount, and $L_{i,k}^{N-1} = \max \{G, W_{i,k}^{N-1}\}$ is the maximal admissible withdrawal amount.

- Following similar procedures, we evaluate GMWB value at time t_n , $n = N-1, N-2, \dots, 1$.

- At $t = 0$, the wealth account value at t_1 can be estimated as

$$\overline{W}_j^1 = W^0 \frac{S_j^1}{S^0} e^{-\alpha \Delta t}, \quad j = 1, \dots, m. \quad (3.12)$$

Similarly, there also exists an integer k^* such that $W_{j,k^*}^1 \leq \overline{W}_j^1 \leq W_{j,k^*+1}^1$. The corresponding GMWB value at t_1 is

$$\overline{V}_j^1 = \lambda_j^1 V_{j,k^*+1}^1 + (1 - \lambda_j^1) V_{j,k^*}^1, \quad (3.13)$$

where

$$\lambda_j^1 = \frac{\overline{W}_j^1 - W_{j,k^*}^1}{W_{j,k^*+1}^1 - W_{j,k^*}^1}.$$

Since there is no withdrawal at the initial time t_0 , the GMWB value at $t_0 = 0$ can be calculated as

$$V^0 = e^{-r \Delta t} \sum_{j=1}^m q_j \overline{V}_j^1, \quad (3.14)$$

where q_j is the transition probability from S^0 to S_j^1 .

The above three-step procedure of pricing GMWB based on the willow tree structure can be summarized in the following algorithm. The inclusion of dynamic withdrawals, mortality risk and surrender will be discussed later.

Algorithm 1 Consider a GMWB expiring in T years with initial investment W^0 and annualized participating fee α . Given the value of the fund $S(t)$ following Merton's jump-diffusion model (2.1) and withdrawal strategy $\{\xi_n\}$, the value of GMWB at initiation (without considering mortality risk and surrender) can be calculated by the willow tree algorithm as follows.

1. Construct the willow tree for the fund value $\{S_i^n\}$ with the transition probabilities $[p_{ij}^n]$ and $\{q_j\}$ from time t_0 to $t_N = T$.
2. Calculate the guaranteed withdrawal account $\{A^n = A(t_n^-)\}$ as in (2.5a) or (2.5b) for $n = 1, 2, \dots, N$; then compute $\{W_{i,\max}^n\}$ as in (3.5) and K possible wealth account values $\{W_{i,k}^n\}$ as in (3.6).
3. Calculate $V_{i,k}^N$ as in (3.7).
4. **for** $n = N - 1 : -1 : 1$
 - for** $i = 1 : m$
 - for** $k = 1 : K$

- for** $j = 1 : m$
 – Calculate \overline{W}_j^{n+1} as in (3.8);
 – Find k^* s.t. $W_{j,k^*}^{n+1} \leq \overline{W}_j^{n+1} \leq W_{j,k^*+1}^{n+1}$ and calculate \overline{V}_j^{n+1} as in (3.9);
end
 – Calculate $V_{i,k}^n$ as in (3.10);
end
end
end
end
 5. **for** $j = 1 : m$
 – Calculate \overline{W}_j^1 as in (3.12);
 – Find k^* such that $W_{j,k^*}^1 \leq \overline{W}_j^1 \leq W_{j,k^*+1}^1$ and calculate \overline{V}_j^1 as in (3.13);
end
 6. Calculate V^0 as in (3.14).

Inclusion of mortality risk and mix withdrawals (with surrender provision)

Mortality is characterized by the probability that the policyholder dies during $(t_{n-1}, t_n]$. In order to simplify the problem, we assume that when the policyholder dies during $(t_{n-1}, t_n]$, the contract will be terminated at t_n and the wealth account value $W(t_n^-)$ will be returned to the beneficiary at t_n . Suppose the policyholder is x_0 years old at the inception of the contract. The probability that the policyholder survives up to time t_n and dies during $(t_n, t_{n+1}]$ is $\Delta t Q_{x_0+t_n}$. In other words, the policyholder's survival probability during $(t_{n-1}, t_n]$ is $1 - \Delta t Q_{x_0+t_n}$. The GMWB value can be rewritten as

$$V_{i,k}^n = e^{-r\Delta t} \left[(1 - \Delta t Q_{x_0+t_n}) \sum_{j=1}^m p_{ij}^n \overline{V}_j^{n+1} + \Delta t Q_{x_0+t_n} \sum_{j=1}^m p_{ij}^n \overline{W}_j^{n+1} \right] + \varphi(\xi_n), \quad (3.15)$$

where \overline{W}_j^{n+1} is the estimated account value at withdrawal date t_{n+1}^- . The value of GMWB at initial time $t_0 = 0$ then can be evaluated as

$$V^0 = e^{-r\Delta t} \left[(1 - \Delta t Q_{x_0}) \sum_{j=1}^m q_j \overline{V}_j^1 + \Delta t Q_{x_0} \sum_{j=1}^m q_j \overline{W}_j^1 \right]. \quad (3.16)$$

Under the mix withdrawals with surrender provision, the policyholder has the option to withdraw the whole wealth account value and terminate the GMWB on a withdrawal date before maturity.

A rational policyholder makes decision on surrender based on the dynamic procedure of finding maximum of the holding value and surrender value. On the withdrawal date t_n , the surrender value $VR_{i,k}^n$ can be calculated as

$$VR_{i,k}^n = \begin{cases} G + (1 - \eta)(W_{i,k}^n - G), & W_{i,k}^n > G, \\ W_{i,k}^n, & W_{i,k}^n \leq G, \end{cases} \quad (3.17)$$

where η is the penalty charge. The GMWB value $V_{i,k}^n$ computed by (3.15) at t_n is visualized as the GMWB holding value, $VC_{i,k}^n$. Based on optimality under mix withdrawal, the GMWB value $V_{i,k}^n$ at t_n is taken to be the maximum of the surrender value and holding value, where

$$V_{i,k}^n = \max \{VC_{i,k}^n, VR_{i,k}^n\}. \quad (3.18)$$

3.3 Numerical valuation framework under dynamic withdrawals

The dynamic withdrawal clause allows the policyholder to choose the withdrawal amounts optimally. In other words, the policyholder decides an optimal withdrawal strategy $\boldsymbol{\xi}^* = \{\xi_1^*, \xi_2^*, \dots, \xi_N^*\}$ to maximize the present value of the GMWB V^0 , where

$$\boldsymbol{\xi}^* = \operatorname{argmax}_{\boldsymbol{\xi} \in P} V^0(S^0, W^0, A^0; \boldsymbol{\xi}). \quad (3.19)$$

Here, P is the set of all admissible withdrawal strategies. The contractual withdrawal amount ξ_n at t_n is up to $\min\{G, A^n\}$. However, when $W^n > \min\{G, A^n\}$, the policyholder is allowed to withdraw more, subject to penalty charge, until the wealth account is completely exhausted. Hence, the admissible value for the withdrawal ξ_n is bounded by $0 \leq \xi_n \leq \max\{W^n, \min\{G, A^n\}\}$. The optimal withdrawal $\boldsymbol{\xi}^*$ can be found by employing dynamic programming procedure on the Bellman recursive equation. Proceeding backward induction in time for $n = N, N - 1, \dots, 1$, we have

$$\begin{aligned} V^{N*}(S^N, W^N, A^N) &= \max\{A^N, W^N\}, \\ V^{n*}(S^n, W^n, A^n) &= \max_{\xi_n \in [0, \max\{W^n, \min\{G, A^n\}\}]} \\ &\quad \mathbb{E}[\varphi(\xi_n) + e^{-r\Delta t} V(S^{n+1}, \overline{W}^{n+1}(\xi_n), \overline{A}^{n+1}(\xi_n)) | S^n, A^n, W^n], \\ V^{0*} &= \mathbb{E}[e^{-r\Delta t} V(S^1, W^1, A^1) | S^0, A^0 = W^0], \end{aligned}$$

where $\overline{W}^{n+1}(\xi_n)$ and $\overline{A}^{n+1}(\xi_n)$ are the updated wealth account value and guaranteed withdrawal account at t_{n+1} , conditional on withdrawal ξ_n at t_n . The above Bellman recursive equation can be solved efficiently by a standard dynamic programming algorithm for a discrete stochastic control problem. Due to our simplistic willow tree structure, the discrete stochastic control problem can

be simplified to successive one-dimensional optimization problems. The global maxima of the constrained optimization problem can be found by the optimization algorithm presented in Appendix B.

The discrete states on $[0, W_{i,\max}^n]$ for W^n and $[0, A^0]$ for A^n at withdrawal date t_n are defined by

$$W_{i,k}^n = \frac{k-1}{K-1} W_{i,\max}^n \quad \text{and} \quad A_h^n = \frac{h-1}{H-1} A^0, \quad k = 1, 2, \dots, K \quad \text{and} \quad h = 1, 2, \dots, H.$$

The GMWB pricing under the dynamic optimization approach can be proceeded as follows:

- On maturity date t_N , the value of GMWB under the dynamic optimization approach V^{N*} can be evaluated as

$$V^{N*}(S_i^N, W_{i,k}^N, A_h^N) = \max \{W_{i,k}^N, A_h^N\}.$$

- On the withdrawal date t_n , $n = N-1, N-2, \dots, 1$, given the withdrawal amount ξ_n at the fund price S_i^n , the wealth account value $W_{i,k}^n$ and guaranteed withdrawal account A_h^n , the GMWB value can be computed as

$$V^n(S_i^n, W_{i,k}^n, A_h^n, \xi_n) = e^{-r\Delta t} \sum_{j=1}^m p_{ij}^n V^{(n+1)*}(S_j^{n+1}, \bar{W}_j^{n+1}, \bar{A}^{n+1}) + \varphi(\xi_n), \quad (3.20)$$

where

$$\bar{W}_j^{n+1} = \max \{W_{i,k}^n - \xi_n, 0\} \frac{S_j^{n+1}}{S_i^n} e^{-\alpha\Delta t},$$

$$\bar{A}^{n+1} = \begin{cases} A_h^n - \xi_n & \xi_n \leq E_h^n \\ \max \left\{ \min \left\{ A_h^n - \xi_n, A_h^n \frac{W_{i,k}^n - \xi_n}{W_{i,k}^n} \right\}, 0 \right\} & \xi_n > E_h^n, \end{cases}$$

and

$$\varphi(\xi_n) = \begin{cases} \xi_n & \xi_n \leq E_h^n \\ E_h^n + (1-\eta)(\xi_n - E_h^n) & \xi_n > E_h^n, \end{cases}$$

with $E_h^n = \min\{G, A_h^n\}$. The GMWB value $V^{(n+1)*}(S_j^{n+1}, \bar{W}_j^{n+1}, \bar{A}^{n+1})$ can be evaluated by the two-dimensional linear interpolation with respect to \bar{W}_j^{n+1} and \bar{A}^{n+1} , where

$$\begin{aligned} & V^{(n+1)*}(S_j^{n+1}, \bar{W}_j^{n+1}, \bar{A}^{n+1}) \\ &= (1-y) \left[xV_{j,k^*+1,h^*}^{(n+1)*} + (1-x)V_{j,k^*,h^*}^{(n+1)*} \right] + y \left[xV_{j,k^*+1,h^*+1}^{(n+1)*} + (1-x)V_{j,k^*,h^*+1}^{(n+1)*} \right]. \end{aligned}$$

The two integers k^* and h^* can be determined as $W_{j,k^*}^{n+1} \leq \bar{W}_j^{n+1} \leq W_{j,k^*+1}^{n+1}$ and $A_{h^*}^{n+1} \leq \bar{A}^{n+1} \leq A_{h^*+1}^{n+1}$, $V_{j,k^*,h^*}^{n*} = V^{n*}(S_j^n, W_{j,k^*}^n, A_{h^*}^n)$, and

$$x = \frac{\bar{W}_j^{n+1} - W_{j,k^*}^{n+1}}{W_{j,k^*+1}^{n+1} - W_{j,k^*}^{n+1}}, \quad \text{and} \quad y = \frac{\bar{A}^{n+1} - A_{h^*}^{n+1}}{A_{h^*+1}^{n+1} - A_{h^*}^{n+1}}.$$

The value of k^* is given by

$$k^* = \left\lceil \frac{(W_{i,k}^n - \xi_n)(K - 1)}{W^0 S_i^n e^{-\alpha n \Delta t}} \right\rceil,$$

independent of S_j^{n+1} . Lastly, we obtain the GMWB value under dynamic withdrawals via

$$V^{n*}(S_i^n, W_{i,k}^n, A_h^n) = \max_{\xi_n \in [0, L_{i,k,h}^n]} V^n(S_i^n, W_{i,k}^n, A_h^n, \xi_n), \quad (3.21)$$

where $L_{i,k,h}^n = \max\{W_{i,k}^n, \min\{A_h^n, G\}\}$. Due to simplicity of the objective function $V^n(S_i^n, W_{i,k}^n, A_h^n, \xi_n)$ in (3.20), the global maximum of (3.21) can be found efficiently by the dynamic optimization algorithm presented in Appendix B. When the mortality risk is included into consideration, the objective function can be modified as

$$\begin{aligned} V^n(S_i^n, W_{i,k}^n, A_h^n, \xi_n) = & e^{-r\Delta t} \left[(1 - \Delta t Q_{x_0+t_n}) \sum_{j=1}^m p_{ij}^n V^{(n+1)*}(S_j^{n+1}, \bar{W}_j^{n+1}, \bar{A}^{n+1}) \right. \\ & \left. + \Delta t Q_{x_0+t_n} \sum_{j=1}^m p_{ij}^n \bar{W}_j^{n+1} \right] + \varphi(\xi_n). \end{aligned}$$

- At the initial time $t_0 = 0$, the GMWB price under dynamic withdrawals can be written as

$$V^{0*} = e^{-r\Delta t} \sum_{j=1}^n q_j V^{1*}(S_j^1, \bar{W}_j^1, \bar{A}^1),$$

since no withdrawal has taken place at the initial time.

4 Numerical studies on pricing behaviors and hedging performance

In this section, we present the numerical studies on numerical accuracy and efficiency of the willow tree algorithm for pricing GMWB under the CEV model, Merton's jump-diffusion model and geometric Brownian motion (nested within the two earlier processes) under static, mix and dynamic withdrawals. The mortality risk is also taken in consideration in our numerical experiments. We compare the performance of our willow tree method (WTM) with other established pricing algorithms, like the bino-trinomial tree method (YDT) (Yang and Dai, 2013), numerical integration method (BMM) (Bacinello *et al.*, 2016), Gauss-Hermite quadrature on cubic spline (GHQC) method (Luo and Shevchenko, 2015), Fourier-cosine (COS) method (Alonso-García *et al.*, 2018) and Monte Carlo (MC) method (Bauer *et al.*, 2008). All experiments were performed on the computer with Intel(R) Core(TM) i7-5600U CPU 2.60GHz processor and 8GB RAM running MATLAB R2016b under Windows 10 Professional.

4.1 Sensitivity analysis of model parameters and comparison of numerical accuracy

First, we investigate the impact of the number of nodes m in the willow tree and number of discrete values K of the wealth account on the values of GMWBs under the geometric Brownian motion (GBM). Figure 2(a) plots the numerical values of the GMWB maturing in 20 years against $1/m$ under varying values of volatility. The risk free interest rate is $r = 3.25\%$ and participating fee is $\alpha = 50\text{bp}$. The plots reveal nice convergence of the numerical results with increasing value of m (equivalently, $1/m$ tends to zero). Similarly, Figure 2(b) reveals the almost linear rate of convergence of the numerical GMWB values with respect to the stepwidth in the wealth account (equivalent to linear rate of convergence in $1/K$). Based on these numerical studies on convergence, we use $m = 100$ and $K = 20$ in our later numerical tests under GBM, unless otherwise stated.

Geometric Brownian motion

There are abundance of numerical results on pricing GMWB in earlier papers that choose the underlying fund dynamics to be the geometric Brownian motion. We compare the performance of our willow tree method (WTM) with YDT (Yang and Dai, 2013), BMM (Bacinello *et al.*, 2016) and Monte Carlo (MC) simulation method on pricing GMWB with various maturities and fund volatilities under static withdrawals. The number of simulation paths used in our Monte Carlo calculations is 10^5 . Figure 3 shows the plot of the GMWB value against varying levels of the participating fee. The parameter values used in the calculations are $T = 20$, $r = 3.25\%$ and $\sigma = 0.2$. The GMWB value decreases by about 10% when we change from zero participating fee to charging participating fee at 100bp. Apparently, the numerical values of GMWB agree reasonably well among the four pricing algorithms. Table 1 records in details the computed GMWB values and the corresponding computing times of these four methods when the participating fee is 50bp. The number of time steps between consecutive withdrawal dates in the YDT method is set to be 50 and 100, respectively. In the BMM method, we let K denote the number of nodes in the discretization of the wealth account, which is set to be $K = 200$ or 300 in our calculations. Numerical tests illustrate that K has to be larger than 200 in order to achieve sufficient numerical accuracy in the BMM method. We also record the average relative errors (RE) of the results using the WTM with $m = 100$ and those from the MC method in Table 1. All computed values obtained from the WTM fall within the 99% confidence interval (CI) of the Monte Carlo simulation results. The willow tree method gives highly accurate results of GMWB values, while requires less computing time when

compared with the YDT, BMM and MC methods, especially for long-maturity GMWB contracts.

We also examine the impact of mortality risk and surrender provision on the fair participating fee to be charged by the issuer of the GMWB. Since mortality risk is not considered in the BMM method, only the YDT method and the willow tree method are compared under the geometric Brownian motion. The policyholder is taken to be a 40-year old male ¹. Table 2 records the computed participating fee α using the willow tree method and YDT method with/without mortality risk and with/without surrender provision. The differences between the numerical values of the fair fees computed by the willow tree method and YDT method are typically small under varying values of maturity and volatility. The willow tree method requires less computing time, especially for long maturity GMWB contracts. The numerical results reveal that the surrender provision plays an important role in determining the fair fee, especially when the underlying fund volatility is high. In our numerical experiments, the penalty charge is set to be $\eta = 10\%$, which is considered to be rather high. When $\sigma = 0.2$, the fair fee with and without surrender provision are almost the same since the surrender provision is not exercised due to high penalty charge. However, the difference in fair fees with and without surrender provision becomes significant when $\sigma = 0.3$. Therefore, managing the risk associated with the surrender provision under more volatile fund dynamics becomes more important, especially for short-maturity GMWB contracts. The mortality risk is another risk factor to be considered in pricing and hedging GMWB. As revealed in Table 2, the mortality risk lowers the fair fee for GMWB, but its influence is negligible when no surrender provision is embedded in the contract. In other words, the surrender provision increases the impact of mortality risk on the fair fee of GMWB, especially when the fund becomes more volatile.

Figure 4 shows the sensitivity of the fair fees under static, mix and dynamic withdrawals with respect to varying levels of penalty charge and maturity when the volatility of the fund dynamics is set at high level of $\sigma = 0.4$. Figure 4(a) shows that the fair fee for the mix and dynamic cases come close to each other under all levels of penalty charge. This implies that the policyholder may focus on the choice of either full surrender or no surrender of the GMWB, rather than making decision on choosing excessive withdrawal beyond G under the dynamic withdrawal case. On the other hand, the difference in fair fees under static and mix withdrawals becomes smaller when η increases. We can deduce that setting high penalty charge is an effective way to hedge against the risk associated with early surrender. Figure 4(b) illustrates that the value of the surrender provision decreases with

¹We adopt the 1994 Group Annuitant Mortality (GAM) Static Table and 1994 Mortality Improvement Projection Scale from the Society of Actuaries Group to estimate the mortality.

longer maturity of the GMWB contract.

Table 3 records the sensitivity of the fair fees with respect to maturity and interest rate computed by the WTM and BMM method under different types of withdrawals. Since the YDT method is not effective to handle the dynamic case, it is excluded in the comparison. Our results show that the fair fee for dynamic withdrawals is higher than the other two types of withdrawals. The fair fees decrease with increasing interest rate r and maturity T . The computation of the fair fee under dynamic withdrawals is quite demanding in the BMM method since a brute force search of the optimal withdrawal amount on each withdrawal date is performed. The willow tree method is more computationally efficient, which only takes a few seconds to compute the fair fee since the algorithm involves an effective optimization method to search for the optimal withdrawal. The two sets of numerical results from the BMM method and WTM do not agree well under the dynamic withdrawal case. However, we believe that the WTM results are more trustworthy than those of the BMM method. To illustrate numerical accuracy of the WTM, we compare the WTM results with those of the GHQC (Luo and Shevchenko, 2015) method and COS (Alonso-García *et al.*, 2018) method. The contractual terms in the GMWB contracts discussed in GHQC (Luo and Shevchenko, 2015) and COS (Alonso-García *et al.*, 2018) method show some small differences from ours. The details of these differences are listed in Table 4.

Tables 5 and 6 show the computed fair fees for the GMWB contracts as specified in Alonso-García *et al.* (2018) by the WTM, GHQC and COS methods. These numerical results reveal good accuracy of the willow tree method when compared with the GHQC and COS methods. The BMM method is not included in both tables since numerical results using the BMM method are not available under these GMWB contractual terms. The fair fees increase with higher frequency of withdrawals per year and decreasing penalty charge η .

Finally, Table 7 records the computed GMWB values and the computational times for static withdrawals with respect to the number of nodes in the willow tree m and number of discrete values of the wealth account K . The benchmark value of the GMWB is 100. The computational time increases approximately superlinear in m and K .

CEV model

Since available numerical algorithms reported in the literature have not been applied to the CEV model, we compare the numerical results using our willow tree method with those from the MC method under static withdrawal and participating fee of 50bp. Table 8 records the GMWB values

computed by the WTM and MC method. All computed values from the WTM fall within 99% confidence level of the MC method, which reveal good accuracy of our willow tree method. We also check the impact of the surrender provision and mortality risk on the fair fees (see Table 9). Similar to the geometric Brownian motion case, the surrender provision is seen to play a key role in determining the fair fee, especially under high volatility of the fund dynamics. We observe that the fair fees are not quite sensitive to the constant elasticity of variance parameter β under all types of withdrawals (see Table 10).

Merton's jump-diffusion model

We compare the performance of the willow tree method with the BMM method under Merton's jump-diffusion model. First, we verify numerical accuracy of the willow tree method by comparing the computed fair fee of GMWB under the jump-diffusion model with the method in Huang *et al.* (2012). Table 11 illustrates that the fair fees of GMWB computed by the two methods are very close to each other. Next, we show the fair fees of GMWB computed by the WTM and BMM method under static, mix and dynamic withdrawals in Tables 12 and 13. Similarly, the fair fee decreases as the interest rate increases, so interest rate is an important risk factor for GMWB contracts with long maturities. As observed from Table 13, when the penalty charge increases, both the fair fees for the mix and dynamic withdrawals converge to those under the static case. In other words, the policyholder is reluctant to surrender at a high penalty charge. This shows that the penalty charge is an important factor for the insurer to mitigate the risk associated with the surrender provision in GMWB. Since the BMM method computes the fair fees under dynamic withdrawals without implementing effective search algorithm for finding optimal withdrawals, the reported numerical results do not exhibit reasonable level of accuracy.

In a typical GMWB contract, the penalty charge η is time-dependent and decreases as time progresses during the life of the contract. Table 14 shows a typical specification for the penalty charge, which starts at the level of 3.0% in the first 5 years then decreases in steps and down to 1.5% in the last 5 years. The corresponding GMWB fair fees for the static, mix and dynamic withdrawals are recorded in Table 14. Compared with the fair fees with a constant penalty $\eta = 3\%$ shown in Table 13, the GMWB fair fee with a decreasing penalty increase insignificantly. This is in agreement with the findings in Chen *et al.* (2008).

Figure 5 shows the sensitivity of the GMWB value with respect to varying levels of the participating fee under static, mix and dynamic withdrawals. When the participating fee is small, the

GMWB values under the static and mix withdrawals are almost same, implying that the policyholder tends not to exercise the surrender provision even when the penalty is only 2%. On the other hand, when a high participating fee is charged, the GMWB values decrease slowly with increasing fee, implying that the policyholder has higher potential to exercise the surrender provision.

4.2 Delta hedging efficiency

We consider delta hedging efficiency under Merton's jump-diffusion model. The delta hedging portfolio consists of long position of the underlying fund, bank account and short position of the GMWB contract. The portfolio value $\Pi(t)$ is given by

$$\Pi(t) = \Delta_S(t)S(t) + \Delta_B(t)B(t) - V(t). \quad (4.1)$$

Here, $\Delta_S(t)$ and $\Delta_B(t)$ are the holding position of underlying asset fund and the value in bank account, respectively. The delta for the GMWB contract on the withdrawal date t_n is defined by

$$\Delta_S(t_n) = \frac{W(t_n)}{S(t_n)} \frac{\partial V}{\partial W},$$

which is computed numerically using the finite difference approximation in our numerical calculations. In our numerical tests, we execute delta hedging only on the withdrawal dates. Figures 6 and 7 show the histograms of the relative realized profit and loss distribution with and without executing the delta hedging strategies under various levels of jump risks computed using Monte Carlo simulation using 1000 simulation paths. Figure 6 illustrates effectiveness of delta hedging on various levels of jump intensity λ . When the intensity is small, such as $\lambda = 0.5282, 1$ or 2 , delta hedging works well in reducing the risk. The relative realized profit and loss is sufficiently close to zero. When the jump intensity becomes larger, like $\lambda = 5$, the relative profit and loss distribution is clustered around -0.3% . When the jump risk is significant, delta hedging procedure is not sufficient. Other derivatives, like options on the asset fund, may be added into the portfolio to improve the hedging performance. Figure 7 illustrates the hedging performance on various σ_J 's with a fixed λ . As σ_J increases, effectiveness of delta hedging declines quite slowly. In other words, σ_J has less influence on the hedging performance when compared with that of λ .

5 Conclusion

Pricing and hedging of the GMWB rider in variable annuities are challenging due to the sophisticated structural features associated with dynamic withdrawals, reset provisions upon excessive

withdrawal, surrender provision and mortality. We propose the willow tree algorithms for pricing GMWB when the underlying fund process follows Merton's jump-diffusion model or CEV model. Unlike the usual lattice tree algorithm and finite difference method, the willow tree algorithm adopts more effective placement of the lattice nodes based on better fitting of the underlying fund price distribution. The willow tree construction can be performed under different choices of the fund price dynamics, and it can be separated from the part of the algorithm that deals with dynamic withdrawals, reset and surrender event on withdrawal dates. We also propose an effective optimization algorithm for the determination of optimal withdrawals. Extensive numerical tests were conducted to examine numerical performance of the willow tree algorithm when compared with other numerical algorithms, like the binomial tree method, finite difference method, numerical quadrature and Fourier transform algorithm. These tests reveal high accuracy, efficiency and reliability of the willow tree algorithm, together with significant savings on computational time. We performed comprehensive sensitivity analysis of various model parameters on the fair participating fees and values of GMWB products, like maturity of the contract, volatility of the fund dynamics, participating fee, penalty charge, etc. We also examine the impact of the jump intensity and magnitude on the terminal profit and loss distribution of the GMWB product with and without delta hedging. The potential losses under strong jumps can be significant under no delta hedging of the GMWB product.

References

- Alonso-García, J., Wood, O. and Ziveyi, J. (2018). Pricing and hedging guaranteed minimum withdrawal benefits under a general Lévy framework using the COS method. *Quantitative Finance*, **18(6)**, 1049-1075.
- Azimzadeh, P. and Forsyth, P.A. (2015). The existence of optimal bang-bang controls for GMxB contracts. *SIAM Journal on Financial Mathematics*, **6(1)**, 117-139.
- Bacinello, A.R., Millossovich, P. and Montealegre, A. (2016). The valuation of GMWB variable annuities under alternative fund distributions and policyholder behaviours. *Scandinavian Actuarial Journal*, 446-465.
- Ballotta, L. and Kyriakou, I. (2015). Convertible bond valuation in a jump diffusion setting with stochastic interest rates. *Quantitative Finance*, **15**, 115-129.
- Bauer, D., Kling, A. and Russ, J. (2008). A universal pricing framework for guaranteed minimum benefits in variable annuities. *Astin Bulletin*, **38**, 621-651.
- Chen, Z., Vetzal, K. and Forsyth, P. (2008). The effect of modeling parameters on the value of GMWB guarantees. *Insurance: Mathematics and Economics*, **43**, 165-173.
- Costabile, M. (2017). A lattice-based model to evaluate variable annuities with guaranteed minimum withdrawal benefits under a regime-switching model. *Scandinavian Actuarial Journal*, 231-244.
- Cox, J. (1975). Notes on option pricing I: Constant elasticity of diffusions. *Working paper of Stanford University*.
- Cox, J., Ingersoll, J. and Ross, S. (1985). A theory of the term structure of interest rates. *Econometrica*, **53(2)**, 385-407.
- Curran, M. (2001). Willow power: optimizing derivative pricing trees. *Algo Research Quarterly*, **4**, 15-24.
- Dai, M., Kwok, Y.K. and Zong, J. (2008). Guaranteed minimum withdrawal benefit in variable annuities. *Mathematical Finance*, **18**, 595-611.
- Forsyth, P. and Vetzal, K. (2014). An optimal stochastic control framework for determining the cost of hedging of variable annuities. *Journal of Economic Dynamics and Control*, **44**, 29-53.
- Geman, H. and Shih, Y.F. (2009). Modeling commodity prices under the CEV model. *Journal of Alternative Investments*, **11**, 65-84.

- Gudkov, N., Ignatieva, K. and Ziveyi, J. (2018). Pricing of GMWB options in variable annuities under stochastic volatility, stochastic interest rates and stochastic mortality via the componentwise splitting method. To appear in *Quantitative Finance*.
- Hill, I. and Holder, R. (1976). Algorithm as 99: Fitting Johnson curves by moments. *Applied Statistics*, **25**, 180-189.
- Huang, Y.Q., Forsyth, P.A. and Labahn, G. (2012). Iterative methods for the solution of a singular control formulation of a GMWB pricing problem. *Numerische Mathematik*, **122**, 133-167.
- Huang, Y.Q. and Forsyth, P.A. (2012). Analysis of a penalty method for pricing a guaranteed minimum withdrawal benefit (GMWB). *Journal of Numerical Analysis*, **32**, 320-351.
- Huang, Y.T. and Kwok, Y.K. (2014). Analysis of optimal withdrawal policies in withdrawal guarantee products. *Journal of Economic Dynamics and Control*, **45**, 320-351.
- Ignatieva, K., Song, A. and Ziveyi, J. (2016). Pricing and hedging of guaranteed minimum benefits under regime-switching and stochastic mortality. *Insurance: Mathematics and Economics*, **70**, 286-300.
- Johnson, N. (1949). System of frequency curves generated by methods of translation. *Biometrika*, **36**, 149-176.
- Kang, B. and Ziveyi, J. (2018). Optimal surrender of guaranteed minimum maturing benefits under stochastic volatility and interest rates. *Insurance: Mathematics and Economics*, **79**, 43-56.
- Lu, L. and Xu, W. (2017). A simple and efficient two-factor willow tree method for convertible bond pricing with stochastic interest rate and default risk. *Journal of Derivatives*, **25**, 37-54.
- Lu, L., Xu, W. and Qian, Z. (2017). Efficient convergent lattice method for Asian options pricing with superlinear complexity. *Journal of Computational Finance*, **20**, 1-38.
- Luo, X. and Shevchenko, P.V. (2015). Valuation of variable annuities with guaranteed minimum withdrawal and death benefits via stochastic control optimization. *Insurance: Mathematics and Economics*, **62**, 5-15.
- Merton, R.C. (1976). Option pricing when underlying stock returns are discontinuous. *Journal of Financial Economics*, **3**, 125-144.
- Milevsky, M. and Salisbury, T. (2006). Financial valuation of guaranteed minimum withdrawal benefits. *Insurance: Mathematics and Economics*, **38**, 21-38.

- Moenig, T. and Bauer, D. (2011). Revisiting the risk-neutral approach to optimal policyholder behavior: A study of withdrawal guarantees in variable annuities. *Working paper in the 12th Symposium on Finance, Banking, and Insurance, Germany*.
- Peng, J.J., Leung, K.S. and Kwok, Y.K. (2012). Pricing guaranteed minimum withdrawal benefits under stochastic interest rates. *Quantitative Finance*, **12**(6), 933-941.
- Shevchenko, P.V. and Luo, X.L. (2017). Valuation of variable annuities with guaranteed minimum withdrawal benefit under stochastic interest rate. *Working paper of Macquarie University*.
- Wang, G. and Xu, W. (2018). A unified willow tree framework for one-factor short rate models. *The Journal of Derivatives*, **25**, 33-54.
- Xu, W., Hong, Z. and Qin, C. (2013). A new sampling strategy willow tree method with application to path-dependent option pricing. *Quantitative Finance*, **13**, 861-872.
- Xu, W. and Yin, Y. (2014). Pricing American options by willow tree method under jump-diffusion process. *Journal of Derivatives*, **22**, 1-9.
- Yang, S.S. and Dai, T.S. (2013). A flexible tree for evaluating guaranteed minimum withdrawal benefits under deferred life annuity contracts with various provisions. *Insurance: Mathematics and Economics*, **52**, 231-242.
- Yao, Y., Xu, W. and Kwok, Y.K. (2019). Willow tree algorithms for pricing exotic derivatives on discrete realized variance under time-changed Lévy process. *Working paper of Tongji University*.

Appendix A - Construction of the willow tree under the CEV process

The asset fund dynamics $S(t)$ that follows the CEV process under a risk neutral measure Q is governed by

$$dS(t) = rS(t)dt + \sigma S(t)^\beta dB(t), \quad (\text{A.1})$$

where r is the risk free interest rate, $B(t)$ is the standard Brownian motion under Q , σ is a constant and β ($\beta > 0$, $\beta \neq 1$) is the constant elasticity of variance parameter. To construct the willow tree for the CEV model, we introduce a new variable $X(t)$ defined by

$$X(t) = S(t)^\theta. \quad (\text{A.2})$$

From the Itô lemma, we can rewrite eq. (A.1) as

$$dX(t) = \theta \left[rX(t) + \frac{\theta - 1}{2} \sigma^2 X(t)^{\frac{\theta - 2(1 - \beta)}{\theta}} \right] dt + \theta \sigma X(t)^{\frac{\theta - (1 - \beta)}{\theta}} dB(t).$$

When $\theta = 2(1 - \beta)$, we have

$$dX(t) = \theta \left[\frac{\theta - 1}{2} \sigma^2 + rX(t) \right] dt + \theta \sigma \sqrt{X(t)} dB(t), \quad (\text{A.3})$$

which reveals that $X(t)$ follows a Cox-Ingersoll-Ross (CIR) process (Cox *et al.*, 1985). Based on the procedure discussed in Wang and Xu (2018), we can construct a willow tree of $X(t)$ governed by the CIR process in eq. (A.3). Given the first four moments of $X(t_n)$ on the withdrawal date t_n , its m possible values X_i^n , $i = 1, 2, \dots, m$, can be estimated by the Johnson curve transformation. The corresponding m asset fund values S_i^n are then given by

$$S_i^n = (X_i^n)^{\frac{1}{\theta}}, \text{ for } i = 1, 2, \dots, m, \text{ and } n = 1, 2, \dots, N.$$

The transition probability p_{ij}^n from S_i^n to S_j^{n+1} can be calculated by

$$p_{ij}^n = P(S_j^{n+1} | S_i^n) = \frac{1}{\sqrt{2\pi[\sigma(S_i^n)^\beta]^2 \Delta t}} \int_A^B \exp\left(-\frac{(x - S_i^n - rS_i^n \Delta t)^2}{2[\sigma(S_i^n)^\beta]^2 \Delta t}\right) dx,$$

where $A = (S_{j-1}^{n+1} + S_j^{n+1})/2$ and $B = (S_{j+1}^{n+1} + S_j^{n+1})/2$. Given the values $\{S_i^n\}$ for $i = 1, 2, \dots, m$ and $n = 1, 2, \dots, N$, and the transition probability matrix $[p_{ij}^n]$, a willow tree can be constructed to approximate the CEV process in eq. (A.1).

Geometric Brownian motion

When $\beta = 1$, the CEV model reduces to the usual geometric Brownian motion. The underlying dynamics of $S(t_n)$ has the explicit analytic form:

$$S(t_n) = S(0)e^{(r - \frac{\sigma^2}{2})t_n + \sigma B(t_n)}.$$

The discrete unit value S_i^n on the willow tree nodes can be estimated as

$$S_i^n = S^0 e^{(r - \frac{\sigma^2}{2})t_n + \sigma\sqrt{t_n}z_i}, \quad \text{for } i = 1, 2, \dots, m,$$

where z_i is the discrete value chosen from the standard normal distribution. Furthermore, the transition probability p_{ij}^n from S_i^n to S_j^{n+1} can be simplified as

$$p_{ij}^n = P(Y_j^{n+1}|Y_i^n) = \int_a^b f(y|Y_i^n) dy, \quad \text{for } i, j = 1, 2, \dots, m,$$

where $Y_i^n = \sqrt{t_n}z_i$, $a = (Y_j^{n+1} + Y_{j-1}^{n+1})/2$, $b = (Y_{j+1}^{n+1} + Y_j^{n+1})/2$. Also, $f(y|Y_i^n)$ is the conditional probability density function given Y_i^n , where

$$f(y|Y_i^n) = \frac{1}{\sqrt{2\pi\Delta t}} \exp\left(-\frac{(y - Y_i^n)^2}{2\Delta t}\right), \quad n = 1, 2, \dots, N - 1.$$

In the first step of the willow tree construction, the transition probability q_i from S^0 to S_j^1 can be determined by

$$q_j = P(Y_j^1|Y^0) = \int_a^b f(y) dy,$$

where $Y_j^1 = \sqrt{\Delta t}z_j$, $a = (Y_j^1 + Y_{j-1}^1)/2$, $b = (Y_{j+1}^1 + Y_j^1)/2$ and $f(y) = \frac{1}{\sqrt{2\pi\Delta t}} \exp(-\frac{y^2}{2\Delta t})$.

Appendix B - Dynamic optimization algorithm in search for optimal withdrawals

In order to solve the optimization problem of finding the optimal withdrawal, the partial derivative of $V^n(S_i^n, W_{i,k}^n, A_h^n, \xi_n)$ with respect to ξ_n can be computed as

$$\frac{\partial V^n}{\partial \xi_n} = e^{-r\Delta t} \sum_{j=1}^m p_{ij}^n \left(\frac{\partial V^{(n+1)*}}{\partial \bar{W}_j^{n+1}} \frac{\partial \bar{W}_j^{n+1}}{\partial \xi_n} + \frac{\partial V^{(n+1)*}}{\partial \bar{A}^{n+1}} \frac{\partial \bar{A}^{n+1}}{\partial \xi_n} \right) + \frac{\partial \varphi}{\partial \xi_n}. \quad (\text{B.1})$$

Since $V^{(n+1)*}(S_j^{n+1}, \bar{W}_j^{n+1}, \bar{A}^{n+1})$ is calculated by the two-dimensional linear interpolation, the corresponding partial derivatives with respect to \bar{W}_j^{n+1} and \bar{A}^{n+1} are given by

$$\begin{aligned} \frac{\partial V^{(n+1)*}}{\partial \bar{W}_j^{n+1}} &= \frac{y \left(V_{j,k^*+1,h^*+1}^{(n+1)*} - V_{j,k^*,h^*+1}^{(n+1)*} \right) + (1-y) \left(V_{j,k^*+1,h^*}^{(n+1)*} - V_{j,k^*,h^*}^{(n+1)*} \right)}{W_{j,k^*+1}^{n+1} - W_{j,k^*}^{n+1}} \\ &= \frac{K-1}{W^0 S_j^{n+1} e^{-(n+1)\alpha\Delta t}} \left[y \left(V_{j,k^*+1,h^*+1}^{(n+1)*} - V_{j,k^*,h^*+1}^{(n+1)*} \right) + (1-y) \left(V_{j,k^*+1,h^*}^{(n+1)*} - V_{j,k^*,h^*}^{(n+1)*} \right) \right] \end{aligned}$$

and

$$\begin{aligned} \frac{\partial V^{(n+1)*}}{\partial \bar{A}^{n+1}} &= \frac{x \left(V_{j,k^*+1,h^*+1}^{(n+1)*} - V_{j,k^*+1,h^*}^{(n+1)*} \right) + (1-x) \left(V_{j,k^*,h^*+1}^{(n+1)*} - V_{j,k^*,h^*}^{(n+1)*} \right)}{A_{h^*+1}^{n+1} - A_{h^*}^{n+1}} \\ &= \frac{H-1}{A_0} \left[x \left(V_{j,k^*+1,h^*+1}^{(n+1)*} - V_{j,k^*+1,h^*}^{(n+1)*} \right) + (1-x) \left(V_{j,k^*,h^*+1}^{(n+1)*} - V_{j,k^*,h^*}^{(n+1)*} \right) \right], \end{aligned}$$

respectively. Putting the results together, $\frac{\partial V^n}{\partial \xi_n}$ in eq. (B.1) on the withdrawal date t_n and at the level of the account value $W_{i,k}^n$ and guaranteed withdrawal account A_h^n , becomes

$$\begin{aligned} \frac{\partial V^n}{\partial \xi_n} = & - e^{-r\Delta t} \sum_{j=1}^m p_{ij}^n \left\{ \frac{a(K-1)}{W^0 S_i^n e^{-n\alpha\Delta t}} \left[\left(V_{j,k^*+1,h^*}^{(n+1)*} - V_{j,k^*,h^*}^{(n+1)*} \right) \right. \right. \\ & + \left. \left(\frac{(H-1)\bar{A}^{n+1}}{A_0} - h^* + 1 \right) \left(V_{j,k^*+1,h^*+1}^{(n+1)*} - V_{j,k^*,h^*+1}^{(n+1)*} - V_{j,k^*+1,h^*}^{(n+1)*} + V_{j,k^*,h^*}^{(n+1)*} \right) \right] \\ & + \frac{b(H-1)}{A_0} \left[\left(V_{j,k^*,h^*+1}^{(n+1)*} - V_{j,k^*,h^*}^{(n+1)*} \right) \right. \\ & + \left. \left. \left(\frac{(K-1)\bar{W}_j^{n+1}}{W_j^0 S_j^{n+1} e^{-(n+1)\alpha\Delta t}} - k^* + 1 \right) \left(V_{j,k^*+1,h^*+1}^{(n+1)*} - V_{j,k^*+1,h^*}^{(n+1)*} - V_{j,k^*,h^*+1}^{(n+1)*} + V_{j,k^*,h^*}^{(n+1)*} \right) \right] \right\} \\ & + c, \end{aligned} \tag{B.2}$$

where

$$a = \begin{cases} 1 & \xi_n < W_{i,k}^n \\ 0 & \xi_n > W_{i,k}^n \end{cases}, \quad b = \begin{cases} \frac{A_h^n}{W_{i,k}^n} & G < \xi_n < W_{i,k}^n < A_h^n \\ 0 & \xi_n > A_h^n \\ 1 & \text{otherwise} \end{cases}, \quad \text{and} \quad c = \begin{cases} 1 & \xi_n \leq E_h^n \\ 1 - \eta & \xi_n > E_h^n \end{cases}.$$

It is seen that $\frac{\partial V^n}{\partial \xi_n}$ in eq. (B.2) is a piecewise linear function of ξ_n . We consider the set of admissible withdrawals ξ_n , which reduce the wealth account value $W_{i,k}^n$ to $W_{j,k'}^{n+1}$, and the guaranteed withdrawal account A_h^n to $A_{h'}^{n+1}$, $k' = 1, 2, \dots, K$ and $h' = 1, 2, \dots, H$. By observing

$$\xi_n = W_{i,k}^n - \frac{W_{j,k'}^{n+1} S_i^n}{S_j^{n+1} e^{-\alpha\Delta t}} = W_{i,k}^n - \frac{(k' - 1) W_{j,\max}^{n+1} S_i^n}{(K - 1) S_j^{n+1} e^{-\alpha\Delta t}} = W_{i,k}^n - \frac{(k' - 1) W_{i,\max}^n}{(K - 1)} = W_{i,k}^n - W_{i,k'}^n$$

and $A_{h'}^n$ is same as $A_{h'}^{n+1}$, these two sets of ξ_n are defined by

$$\Sigma_1 = \{ \xi_n | \xi_n = W_{i,k}^n - W_{i,k'}^n, k' = 1, 2, \dots, K \},$$

and

$$\Sigma_2 = \{ \xi_n | \xi_n = A_h^n - A_{h'}^n, h' = 1, 2, \dots, H \}.$$

Thus, $\frac{\partial V^n}{\partial \xi_n}$ is a linear function with respect to ξ_n in each interval $[\xi_n^l, \xi_n^{l+1}]$, where $\xi_n^l \in \Phi$, $\Phi \equiv \Sigma_1 \cup \Sigma_2$ and $\xi_n^1 < \xi_n^2 < \dots < \xi_n^d$ ($d \leq K + H$).

Given the triplet $(G, W_{i,k}^n, A_h^n)$ and the admissible withdrawal range for ξ_n , we can find the local maximal withdrawal ξ_n^{l*} in each interval $[\xi_n^l, \xi_n^{l+1}]$ as

$$\xi_n^{l*} = \begin{cases} \frac{|y_l| \xi_n^{l+1} + |y_{l+1}| \xi_n^l}{|y_l| + |y_{l+1}|} & y_l > 0 \text{ and } y_{l+1} < 0 \\ \xi_n^l \text{ or } \xi_n^{l+1} & \text{otherwise} \end{cases}, \tag{B.3}$$

where

$$y_l = \left. \frac{\partial V^n}{\partial \xi_n} \right|_{\xi_n = \xi_n^l} \quad \text{and} \quad y_{l+1} = \left. \frac{\partial V^n}{\partial \xi_n} \right|_{\xi_n = \xi_n^{l+1}}.$$

Among these local maxima, we can find the global maximal withdrawal ξ_n^* for $V^n(S_i^n, W_{i,k}^n, A_h^n, \xi_n)$. Since the GMWB value $V^n(S_i^n, W_{i,k}^n, A_h^n, \xi_n)$ can be evaluated by (3.20), the whole searching procedure is very efficient. In fact, given the value of $W_{i,k}^n$ and A_h^n , only a small number of intervals in Φ are required to search for the local minima. In other words, we just need to set up a subset of Φ , denoted by $\tilde{\Phi}$, to determine the searching intervals, given A_h^n , $W_{i,k}^n$ and the admissible withdrawal range of ξ_n . Based on our numerical experiments, we normally use about 8 intervals to determine the optimal withdrawal ξ_n^* .

Next, we show how to set up the subset $\tilde{\Phi}$ for $W_{i,k}^n \leq A_h^n$ and otherwise. Given $W_{i,k}^n \leq A_h^n$, the admissible withdrawal range of ξ_n is $[0, L_{i,k,h}^n]$, where

$$L_{i,k,h}^n = \max \{ W_{i,k}^n, \min \{ A_h^n, G \} \}.$$

There are three cases to be considered in constructing the subset $\tilde{\Phi}$. First, for $\xi_n \in [0, \min \{ G, W_{i,k}^n \}]$, we have

$$\begin{aligned} \frac{\partial V^n}{\partial \xi_n} &= -e^{-r\Delta t} \sum_{j=1}^m p_{ij}^n \left\{ \frac{(K-1)}{W^0 S_i^n e^{-n\alpha\Delta t}} \left[\left(V_{j,k^*+1,h^*}^{(n+1)*} - V_{j,k^*,h^*}^{(n+1)*} \right) \right. \right. \\ &\quad + \left. \left(\frac{(H-1)(A_{h^*}^n - \xi_n)}{A_0} - h^* + 1 \right) \left(V_{j,k^*+1,h^*+1}^{(n+1)*} - V_{j,k^*,h^*+1}^{(n+1)*} - V_{j,k^*+1,h^*}^{(n+1)*} + V_{j,k^*,h^*}^{(n+1)*} \right) \right] \\ &\quad + \frac{(H-1)}{A_0} \left[\left(V_{j,k^*,h^*+1}^{(n+1)*} - V_{j,k^*,h^*}^{(n+1)*} \right) \right. \\ &\quad \left. \left. + \left(\frac{(K-1)(W_{i,k^*}^n - \xi_n)}{W^0 S_i^n e^{-n\alpha\Delta t}} - k^* + 1 \right) \left(V_{j,k^*+1,h^*+1}^{(n+1)*} - V_{j,k^*+1,h^*}^{(n+1)*} - V_{j,k^*,h^*+1}^{(n+1)*} + V_{j,k^*,h^*}^{(n+1)*} \right) \right] \right\} \\ &\quad + 1. \end{aligned}$$

The subset of Φ can be determined as $\tilde{\Phi} = \Phi \cup \{ \min \{ G, W_{i,k}^n \} \} \cap [0, \min \{ G, W_{i,k}^n \}]$.

Second, if $\xi_n \in (W_{i,k}^n, E_h^n]$ and $G \geq W_{i,k}^n$, we have

$$\frac{\partial V^n}{\partial \xi_n} = -e^{-r\Delta t} \sum_{j=1}^m p_{ij}^n \left(\frac{\partial V^{(n+1)*}}{\partial A^{n+1}} \right) + 1.$$

It is easy to show that $\frac{\partial V^{(n+1)*}}{\partial A^{n+1}} \leq 1$. Thus, we have $\left. \frac{\partial V^n}{\partial \xi_n} \right|_{\xi_n \in (W_{i,k}^n, E_h^n]} \geq 0$ since $\sum_{j=1}^m p_{ij}^n = 1$. In other words, V^n is a monotonic increasing function with respect to ξ_n in $(W_{i,k}^n, E_h^n]$. The optimal withdrawal strategy in $(W_{i,k}^n, E_h^n]$ can be determined directly as $\xi_n^* = E_h^n$. As a result, no searching is required.

Finally, if $\xi_n \in (G, W_{i,k}^n]$, we have

$$\begin{aligned} \frac{\partial V^n}{\partial \xi_n} &= -e^{-r\Delta t} \sum_{j=1}^m p_{ij}^n \left\{ \frac{(K-1)}{W^0 S_i^n e^{-n\alpha\Delta t}} \left[\left(V_{j,k^*+1,h^*}^{(n+1)*} - V_{j,k^*,h^*}^{(n+1)*} \right) \right. \right. \\ &\quad + \left(\frac{(H-1)(W_{i,k}^n - \xi_n) A_h^n}{A_0 W_{i,k}^n} - h^* + 1 \right) \left(V_{j,k^*+1,h^*+1}^{(n+1)*} - V_{j,k^*,h^*+1}^{(n+1)*} - V_{j,k^*+1,h^*}^{(n+1)*} + V_{j,k^*,h^*}^{(n+1)*} \right) \\ &\quad + \frac{A_h^n (H-1)}{W_{i,k}^n A_0} \left[\left(V_{j,k^*,h^*+1}^{(n+1)*} - V_{j,k^*,h^*}^{(n+1)*} \right) \right. \\ &\quad \left. \left. + \left(\frac{(K-1)(W_{i,k}^n - \xi_n)}{W^0 S_i^n e^{-n\alpha\Delta t}} - k^* + 1 \right) \left(V_{j,k^*+1,h^*+1}^{(n+1)*} - V_{j,k^*+1,h^*}^{(n+1)*} - V_{j,k^*,h^*+1}^{(n+1)*} + V_{j,k^*,h^*}^{(n+1)*} \right) \right] \right\} \\ &\quad + 1 - \eta. \end{aligned}$$

In this case, since the reset provision is triggered on updating the guaranteed withdrawal amount \bar{A}^{n+1} , the set Σ_2 should be replaced by Σ_3 as follows:

$$\Sigma_3 = \left\{ \xi_n \mid \xi_n = W_{i,k}^n - \frac{W_{i,k}^n A_{h'}^n}{A_h^n}, h' = 1, 2, \dots, H \right\}.$$

Thus, the subset $\tilde{\Phi}$ can be defined as

$$\tilde{\Phi} = \Sigma_1 \cup \Sigma_3 \cup \{W_{i,k}^n\} \cap (G, W_{i,k}^n].$$

Given $W_{i,k}^n > A_h^n$, the admissible withdrawal range is $[0, W_{i,k}^n]$. There are two cases to be considered for setting up the subset $\tilde{\Phi}$, namely, $\xi_n \in [0, A_h^n]$ and $\xi_n \in (A_h^n, W_{i,k}^n]$. When $\xi_n \in [0, A_h^n]$, we have

$$\begin{aligned} \frac{\partial V^n}{\partial \xi_n} &= -e^{-r\Delta t} \sum_{j=1}^m p_{ij}^n \left\{ \frac{(K-1)}{W^0 S_i^n e^{-n\alpha\Delta t}} \left[\left(V_{j,k^*+1,h^*}^{(n+1)*} - V_{j,k^*,h^*}^{(n+1)*} \right) \right. \right. \\ &\quad + \left(\frac{(H-1)(A_h^n - \xi_n)}{A_0} - h^* + 1 \right) \left(V_{j,k^*+1,h^*+1}^{(n+1)*} - V_{j,k^*,h^*+1}^{(n+1)*} - V_{j,k^*+1,h^*}^{(n+1)*} + V_{j,k^*,h^*}^{(n+1)*} \right) \\ &\quad + \frac{(H-1)}{A_0} \left[\left(V_{j,k^*,h^*+1}^{(n+1)*} - V_{j,k^*,h^*}^{(n+1)*} \right) \right. \\ &\quad \left. \left. + \left(\frac{(K-1)(W_{i,k^*}^n - \xi_n)}{W^0 S_i^n e^{-n\alpha\Delta t}} - k^* + 1 \right) \left(V_{j,k^*+1,h^*+1}^{(n+1)*} - V_{j,k^*+1,h^*}^{(n+1)*} - V_{j,k^*,h^*+1}^{(n+1)*} + V_{j,k^*,h^*}^{(n+1)*} \right) \right] \right\} \\ &\quad + c, \end{aligned}$$

where

$$c = \begin{cases} 1, & G \geq A_h^n, \\ 1 \cdot \mathbb{1}_{\{\xi_n \leq G\}} + (1 - \eta) \cdot \mathbb{1}_{\{\xi_n > G\}}, & G < A_h^n. \end{cases}$$

The subset $\tilde{\Phi}$ can be determined as

$$\tilde{\Phi} = \begin{cases} \Phi \cup \{A_h^n\} \cap [0, A_h^n] & G \geq A_h^n \\ \Phi \cup \{G, A_h^n\} \cap [0, A_h^n], & \text{otherwise.} \end{cases}$$

When $\xi_n \in (A_h^n, W_{i,k}^n]$, we have

$$\frac{\partial V^n}{\partial \xi_n} = -e^{-r\Delta t} \sum_{j=1}^m p_{ij}^n \left(e^{-\alpha\Delta t} \frac{S_j^{n+1}}{S_i^n} \frac{\partial V^{(n+1)*}}{\partial W_j^{n+1}} \right) + 1 - \eta,$$

where

$$\frac{\partial V^{(n+1)*}}{\partial \overline{W}_j^{n+1}} = \frac{V_{j,k^{*}+1,1}^{(n+1)*} - V_{j,k^*,1}^{(n+1)*}}{W_{j,k^{*}+1}^{n+1} - W_{j,k^*}^{n+1}} = \frac{(K-1) \left(V_{j,k^{*}+1,1}^{(n+1)*} - V_{j,k^*,1}^{(n+1)*} \right)}{W^0 S_j^{n+1} e^{-(n+1)\alpha\Delta t}}.$$

The subset of Φ is

$$\tilde{\Phi} = \Sigma_1 \cup \{W_{i,k}^n\} \cap (A_h^n, W_{i,k}^n].$$

In summary, the subset $\tilde{\Phi}$ can be constructed as the subset of Φ on the admissible withdrawal range of ξ_n , including the two end points of the admissible range. Once the subset $\tilde{\Phi}$ is determined, the local minima on $[\xi_n^l, \xi_n^{l+1}]$ can be estimated by eq. (B.3). The global optimal withdrawal ξ_n^* is then selected among these local minima.

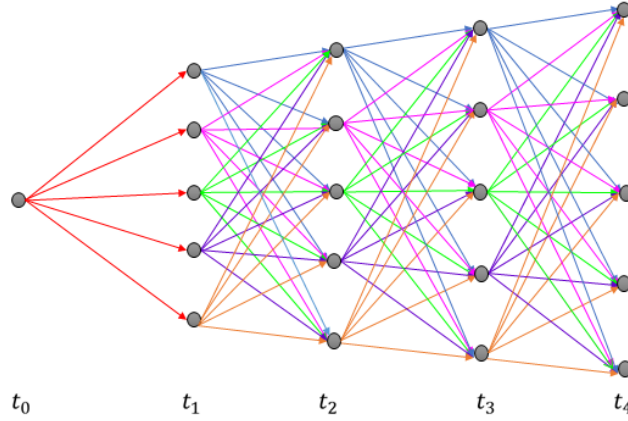
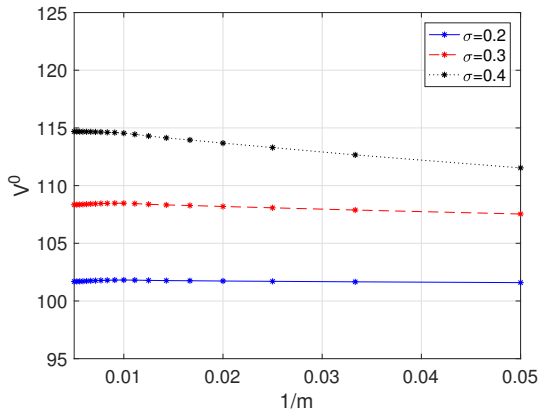
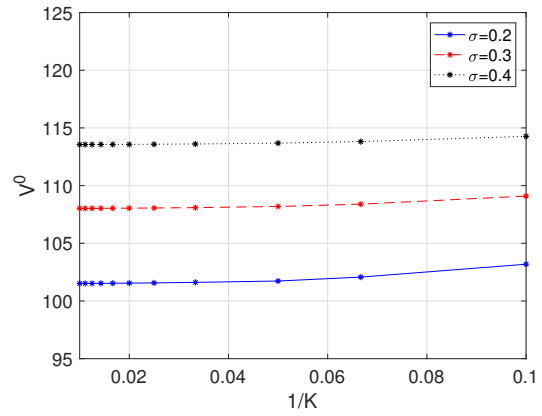


Figure 1: Graphical depiction of the willow tree lattice with 5 space nodes and 4 withdrawal dates.



(a) Plot of V^0 against $1/m$ with $K = 20$ and varying levels of volatility σ .



(b) Plot of V^0 against $1/K$ with $m = 100$ and varying levels of volatility σ .

Figure 2: Convergence of numerical values of the GMWB price under the geometric Brownian motion with respect to the number of nodes m in the willow tree and the number of discrete values of the wealth account value K .

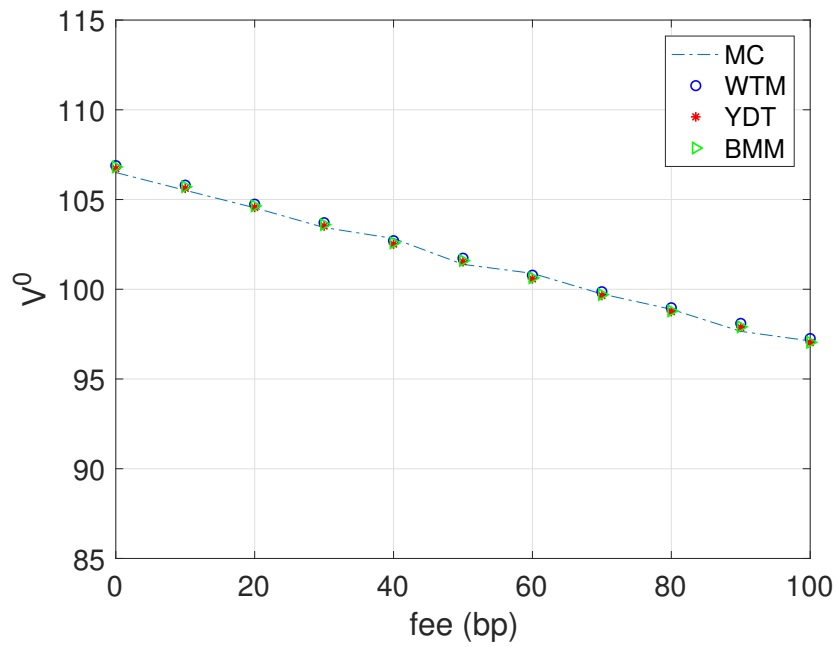
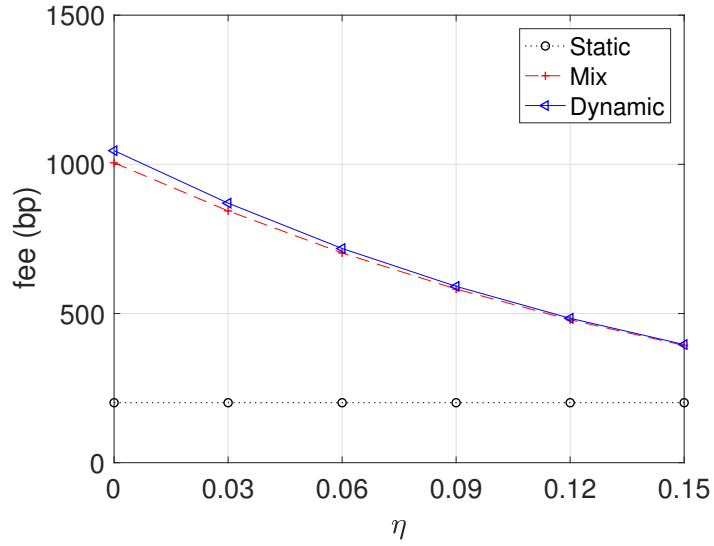
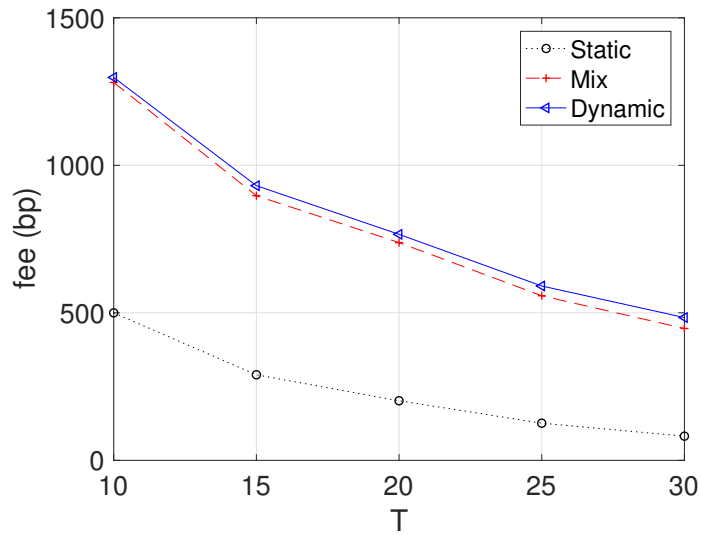


Figure 3: Plot of the GMWB value against varying levels of the participating fee under the geometric Brownian motion and static withdrawal. Good agreement of numerical results is revealed among the four pricing algorithms, WTM, YDT, BMM and MC methods.



(a) Fair fees with respect to penalty η with $T = 20$.



(b) Fair fees with respect to maturity T with $\eta = 5\%$.

Figure 4: Plots of the fair fees of GMWB (in bp) with respect to penalty η and maturity T under the geometric Brownian motion at high volatility level $\sigma = 0.4$ and $r = 3\%$.

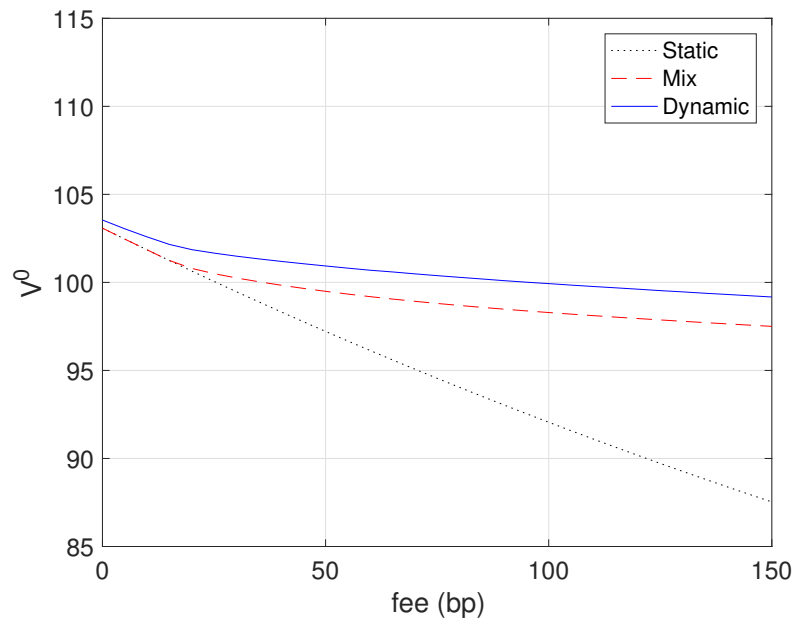
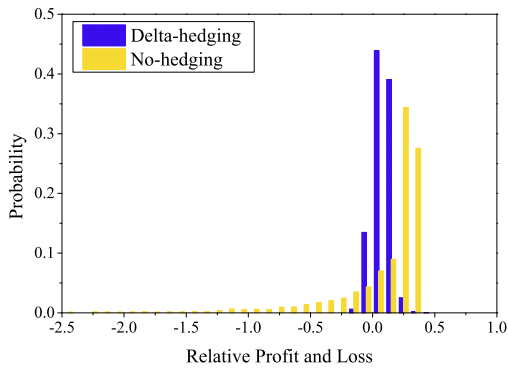
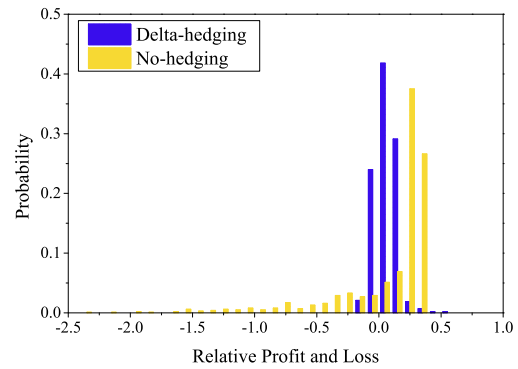


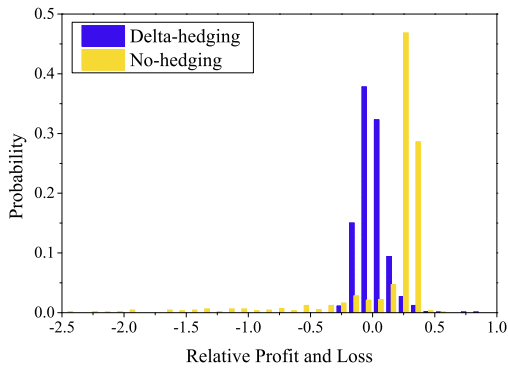
Figure 5: Sensitivity of GMWB value with respect to the participating fee (in bp) under static, mix and dynamic withdrawals. The underlying fund dynamics follows Merton's jump-diffusion models, with $T = 20$, $r = 5\%$, $\sigma_s = 0.1114$, $\alpha_J = -0.1825$, $\sigma_J = 0.1094$, $\lambda = 0.5282$, $\eta = 2\%$.



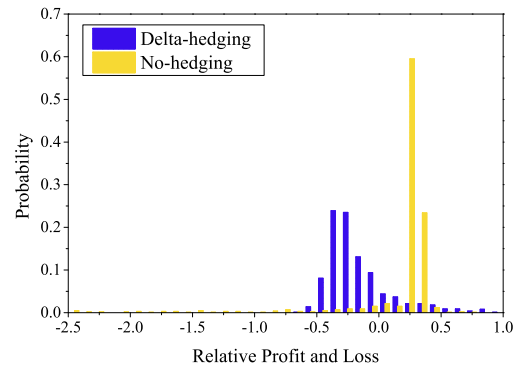
(a) $\lambda = 0.5282$.



(b) $\lambda = 1$.

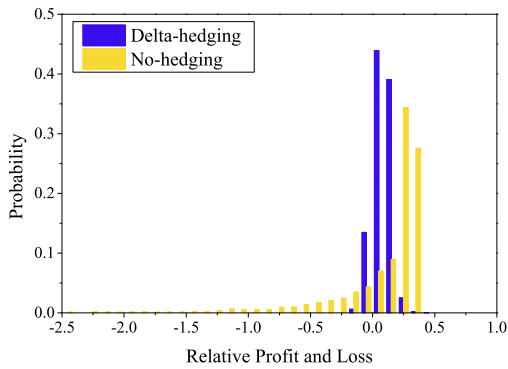


(c) $\lambda = 2$.

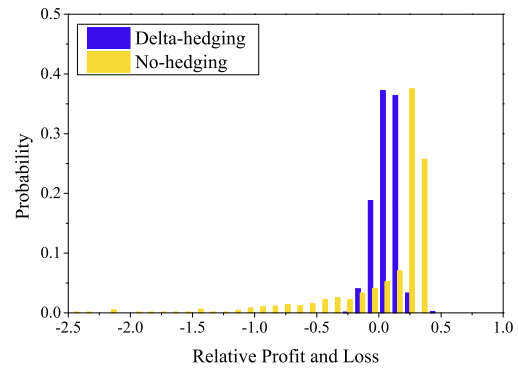


(d) $\lambda = 5$.

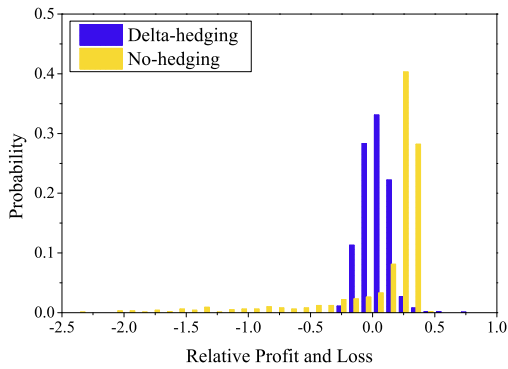
Figure 6: Histogram plots of the profit and loss with and without delta hedging under Merton's jump-diffusion model with varying values of the jump intensity λ . Delta hedging is executed on the withdrawal dates. Parameter values used in the calculations are $T = 20$, $r = 3\%$, $\alpha = 68\text{bp}$, $\sigma = 0.1114$, $\alpha_J = -0.1825$, $\sigma_J = 0.1094$.



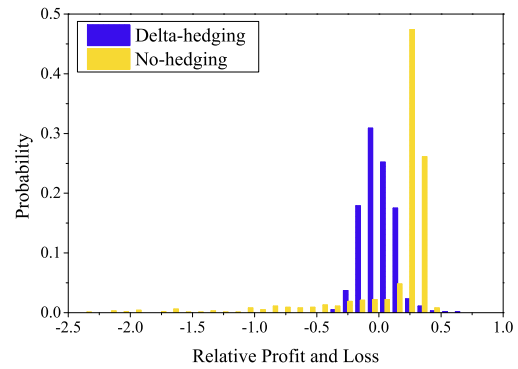
(a) $\sigma_J = 0.1094$.



(b) $\sigma_J = 0.2$.



(c) $\sigma_J = 0.3$.



(d) $\sigma_J = 0.4$.

Figure 7: Histogram plots of the profit and loss with and without delta hedging under Merton's jump-diffusion model using varying values of σ_J . Delta hedging is executed on the withdrawal dates. Parameter values used in the calculations are $T = 20$, $r = 3\%$, $\alpha = 68\text{bp}$, $\sigma = 0.1114$, $\alpha_J = -0.1825$, $\lambda = 0.5282$.

		$T = 10 \quad G = 10$			
		$\sigma = 0.2$		$\sigma = 0.3$	
		V^0	Time(s)	V^0	Time(s)
WTM	m=50	105.174	0.09	111.273	0.09
WTM	m=100	105.269	0.44	111.461	0.42
WTM	m=150	105.264	0.94	111.476	0.91
YDT	N=50T	105.009	0.11	111.183	0.08
YDT	N=100T	105.007	1.02	111.182	0.84
BMM	K=200	105.032	0.70	111.215	0.77
BMM	K=300	105.014	1.25	111.191	1.14
MC	10^5 paths	105.066	6.70	111.142	6.64
	CI (99%)	(104.743, 105.389)		(110.554, 111.730)	
RE		0.19%		0.29%	
		$T = 20 \quad G = 5$			
		$\sigma = 0.2$		$\sigma = 0.3$	
		V^0	Time(s)	V^0	Time(s)
WTM	m=50	101.730	0.23	108.190	0.23
WTM	m=100	101.818	1.16	108.471	0.92
WTM	m=150	101.748	2.06	108.411	1.95
YDT	N=50T	101.536	0.98	108.276	0.72
YDT	N=100T	101.535	7.53	108.275	7.28
BMM	K=200	101.600	3.58	108.593	3.39
BMM	K=300	101.556	4.31	108.437	4.95
MC	10^5 paths	101.616	11.97	108.420	11.92
	CI (99%)	(101.314, 101.918)		(107.978, 108.863)	
RE		0.20%		0.05%	
		$T = 25 \quad G = 4$			
		$\sigma = 0.2$		$\sigma = 0.3$	
		V^0	Time(s)	V^0	Time(s)
WTM	m=50	99.758	0.42	105.937	0.31
WTM	m=100	99.857	1.36	106.340	1.39
WTM	m=150	99.782	2.88	106.298	3.39
YDT	N=50T	99.524	1.91	106.229	1.58
YDT	N=100T	99.524	14.83	106.226	13.30
BMM	K=200	99.649	4.95	106.801	4.625
BMM	K=300	99.569	7.14	106.591	6.578
MC	10^5 paths	99.606	16.17	106.474	14.77
	CI (99%)	(98.754, 100.459)		(105.725, 107.223)	
RE		0.25%		0.13%	

Table 1: Comparison of numerical accuracy of computing GMWB values and required CPU times (in seconds) using four different numerical algorithms under the geometric Brownian motion (without mortality risk and surrender provision). The parameter values used in the calculations are $\alpha = 50\text{bp}$ and $r = 3.25\%$. Here, m is the number of nodes in the willow tree, N is the total number of time steps in YDT and K is the number of nodes in the wealth account.

$T = 20 \quad G = 5$				$\sigma = 0.2$	$\sigma = 0.3$
No Surrender Provision	No Mortality Risk	WTM	m=50	69	141
		WTM	m=100	69	144
		WTM	m=150	69	144
		YDT	N=50T	66	142
		YDT	N=100T	66	142
	With Mortality Risk	WTM	m=50	67	139
		WTM	m=100	68	142
		WTM	m=150	67	141
		YDT	N=50T	65	140
		YDT	N=100T	65	140
With Surrender Provision	No Mortality Risk	WTM	m=50	69	230
		WTM	m=100	69	232
		WTM	m=150	69	228
		YDT	N=50T	66	224
		YDT	N=100T	66	224
	With Mortality Risk	WTM	m=50	67	220
		WTM	m=100	68	222
		WTM	m=150	67	218
		YDT	N=50T	65	215
		YDT	N=100T	65	215
$T = 25 \quad G = 4$				$\sigma = 0.2$	$\sigma = 0.3$
No Surrender Provision	No Mortality Risk	WTM	m=50	48	100
		WTM	m=100	49	103
		WTM	m=150	48	103
		YDT	N=50T	46	102
		YDT	N=100T	46	102
	With Mortality Risk	WTM	m=50	47	97
		WTM	m=100	47	101
		WTM	m=150	47	100
		YDT	N=50T	45	100
		YDT	N=100T	45	100
With Surrender Provision	No Mortality Risk	WTM	m=50	48	164
		WTM	m=100	49	166
		WTM	m=150	48	162
		YDT	N=50T	46	158
		YDT	N=100T	46	158
	With Mortality Risk	WTM	m=50	47	152
		WTM	m=100	47	154
		WTM	m=150	47	151
		YDT	N=50T	45	150
		YDT	N=100T	45	150
$T = 30 \quad G = 10/3$				$\sigma = 0.2$	$\sigma = 0.3$
No Surrender Provision	No Mortality Risk	WTM	m=50	35	73
		WTM	m=100	36	77
		WTM	m=150	36	77
		YDT	N=50T	34	77
		YDT	N=100T	34	77
	With Mortality Risk	WTM	m=50	34	70
		WTM	m=100	35	74
		WTM	m=150	34	74
		YDT	N=50T	33	76
		YDT	N=100T	33	76
With Surrender Provision	No Mortality Risk	WTM	m=50	35	119
		WTM	m=100	36	121
		WTM	m=150	36	118
		YDT	N=50T	34	114
		YDT	N=100T	34	114
	With Mortality Risk	WTM	m=50	34	106
		WTM	m=100	35	108
		WTM	m=150	34	105
		YDT	N=50T	33	106
		YDT	N=100T	33	105

Table 2: Computation of the fair participating fees (in bp) of GMWB under the geometric Brownian motion using the willow tree method (WTM) and lattice tree method (YDT) with/without mortality risk and with/without surrender provision. The differences between the numerical values of the fair fees computed by the two methods are typically small under varying values of maturity and volatility. Parameter values used in the calculations are $r = 3.25\%$ and penalty charge $\eta = 10\%$.

	$T = 20$	r	0.03	0.04	0.05
Static	WTM	Fee (bp)	33	16	8
		Time (s)	3.0	2.7	2.8
	BMM	Fee (bp)	31	15	7
		Time (s)	30.0	32.0	30.1
Mix	WTM	Fee (bp)	33	16	8
		Time (s)	3.5	2.7	2.9
	BMM	Fee (bp)	31	15	8
		Time (s)	33.3	34.3	34.2
Dynamic	WTM	Fee (bp)	81	38	22
	BMM	Fee (bp)	78	27	12
<hr/>					
	$r = 5\%$	T	10	15	20
Static	WTM	Fee (bp)	35	16	8
		Time (s)	1.5	1.6	2.6
	BMM	Fee (bp)	32	14	7
		Time (s)	9.2	17.5	30.5
Mix	WTM	Fee (bp)	35	16	8
		Time (s)	1.3	1.7	2.8
	BMM	Fee (bp)	33	15	8
		Time (s)	8.8	18.9	32.2
Dynamic	WTM	Fee (bp)	49	35	22
	BMM	Fee (bp)	50	24	12

Table 3: Comparison of the fair fees of GMWBs (in bp) and computational times computed by the WTM and BMM method under the geometric Brownian motion with volatility $\sigma = 0.1361$ and penalty charge $\eta = 5\%$. The fair fees decrease with increasing interest rate r and maturity T .

	Reset provision of A^n	Payoff at maturity	Admissible withdrawal at t_n
WTM	reset as in (2.5b)	$\max\{W^N, A^N\}$	$\xi_n \in [0, \max\{W^n, \min\{G, A^n\}\}]$
BMM	reset as in (2.5b)	$\max\{W^N, A^N\}$	$\xi_n \in [0, \max\{W^n, \min\{G, A^n\}\}]$
GHQC	no reset	$\max\{W^N, \varphi(A^N)\}$	$\xi_n \in [0, A^n]$
COS	no reset/reset as in (2.5c)	$\max\{W^N, \varphi(A^N)\}$	$\xi_n \in [0, A^n]$

Table 4: Differences of the GMWB contractual terms between the willow tree method (WTM), BMM (Bacinello *et al.*, 2016), GHQC (Luo and Shevchenko, 2015) and COS (Alonso-García *et al.*, 2018) under dynamic withdrawals.

	$T = 10$	$\sigma = 0.2$	$\sigma = 0.3$
yearly withdrawals	WTM	130	293
	GHQC	129	293
half-yearly withdrawals	WTM	137	303
	GHQC	134	303

Table 5: Comparison of the fair participating fee (bp) computed using the WTM and GHQC with dynamic withdrawals under the geometric Brownian motion. Parameter values are $T = 10$, $r = 5\%$, $\eta = 10\%$. The fair fees increase with higher frequency of withdrawals per year.

T	$\eta = 5\%$			$\eta = 10\%$		
	WTM	COS	GHQC	WTM	COS	GHQC
10	219	217	217	138	136	136
20	124	123	124	72	70	70
25	102	102	102	56	55	56

Table 6: Comparison of the fair participating fee (bp) computed using the WTM, GHQC and COS methods with quarterly dynamic withdrawals under the geometric Brownian motion. Parameter values are $\sigma = 0.2$, $r = 5\%$. The fair fees decrease with increasing penalty charge η .

(a) Geometric Brownian motion					(b) Jump-diffusion model				
$m \backslash K$	10	20	40	80	$m \backslash K$	10	20	40	80
10	100.71 (0.012)	99.64 (0.018)	99.52 (0.025)	99.49 (0.065)	10	101.06 (0.019)	100.10 (0.027)	100.00 (0.030)	99.98 (0.084)
20	100.98 (0.028)	99.91 (0.040)	99.80 (0.100)	99.77 (0.256)	20	100.97 (0.063)	99.99 (0.072)	99.90 (0.130)	99.87 (0.327)
40	101.10 (0.090)	100.03 (0.143)	99.92 (0.341)	99.89 (1.010)	40	100.95 (0.141)	99.98 (0.219)	99.88 (0.425)	99.86 (1.133)
80	101.18 (0.253)	100.11 (0.485)	100.00 (1.295)	99.97 (3.933)	80	100.95 (0.386)	99.98 (0.670)	99.89 (1.511)	99.86 (4.342)
160	101.12 (0.893)	100.06 (2.208)	99.94 (5.332)	99.91 (16.156)	160	100.97 (1.270)	100.00 (2.417)	99.90 (6.052)	99.88 (18.043)
320	101.06 (3.912)	100.00 (8.618)	99.88 (23.936)	99.86 (71.096)	320	100.98 (5.238)	100.01 (10.167)	99.91 (25.410)	99.89 (78.340)

Table 7: Computational times (in seconds) and computed GMWB values under the static withdrawal with varying values of the number of nodes m and discretisation of the investment account K . The computational times are shown in brackets. The GMWB contract matures in 20 years with annual withdrawal. The risk free interest rate r is 5% while the volatility $\sigma = 0.2$ for the geometric Brownian motion. The parameter values for Merton's jump-diffusion model are set to be $\sigma = 0.1114$, $\alpha_J = -0.1825$, $\sigma_J = 0.1094$ and $\lambda = 0.5282$.

		$T = 10$	$G = 10$	$\sigma = 0.2$	$\sigma = 0.3$	$\sigma = 0.4$
$\beta = 0.3$	WTM	m=100		104.761	110.940	117.208
	MC	n=50000		(104.542, 105.202)	(110.778, 111.770)	(116.596, 117.952)
$\beta = 0.5$	WTM	m=100		104.779	111.026	117.442
	MC	n=50000		(104.643, 105.352)	(110.513, 111.621)	(116.257, 117.772)
$\beta = 0.7$	WTM	m=100		104.809	111.154	117.785
	MC	n=50000		(104.492, 105.257)	(110.425, 111.662)	(116.357, 118.173)
		$T = 20$	$G = 5$	$\sigma = 0.2$	$\sigma = 0.3$	$\sigma = 0.4$
$\beta = 0.3$	WTM	m=100		101.066	107.831	114.638
	MC	n=50000		(100.727, 101.615)	(107.602, 108.919)	(114.500, 116.290)
$\beta = 0.5$	WTM	m=100		101.031	107.813	114.712
	MC	n=50000		(101.129, 102.117)	(107.136, 108.656)	(113.625, 115.732)
$\beta = 0.7$	WTM	m=100		100.990	107.765	114.736
	MC	n=50000		(100.697, 101.803)	(106.781, 108.587)	(113.374, 116.151)
		$T = 25$	$G = 4$	$\sigma = 0.2$	$\sigma = 0.3$	$\sigma = 0.4$
$\beta = 0.3$	WTM	m=100		98.986	105.691	112.437
	MC	n=50000		(98.933, 99.893)	(105.667, 107.105)	(112.214, 114.147)
$\beta = 0.5$	WTM	m=100		98.914	105.594	112.380
	MC	n=50000		(98.840, 99.917)	(105.403, 107.075)	(110.412, 112.700)
$\beta = 0.7$	WTM	m=100		98.814	105.398	112.124
	MC	n=50000		(98.582, 99.815)	(104.381, 106.413)	(111.421, 114.506)

Table 8: Computed values of GMWB under the CEV model without mortality risk and surrender provision computed using the willow tree method (WTM). Here, m is the number of nodes in the willow tree and n is the number of Monte Carlo simulation paths. The corresponding 99% confidence level is obtained from the Monte Carlo calculations.

		$T = 10$	$G = 10$	$\sigma = 0.2$	$\sigma = 0.3$	$\sigma = 0.4$
$\beta = 0.3$	No Surrender Provision	No Mortality Risk		161	310	456
		With Mortality Risk		159	308	453
	With Surrender Provision	No Mortality Risk		161	430	853
		With Mortality Risk		159	422	838
$\beta = 0.5$	No Surrender Provision	No Mortality Risk		163	318	472
		With Mortality Risk		161	315	468
	With Surrender Provision	No Mortality Risk		163	439	866
		With Mortality Risk		162	431	851
$\beta = 0.7$	No Surrender Provision	No Mortality Risk		167	333	504
		With Mortality Risk		164	325	488
	With Surrender Provision	No Mortality Risk		165	450	886
		With Mortality Risk		164	443	871
		$T = 20$	$G = 5$	$\sigma = 0.2$	$\sigma = 0.3$	$\sigma = 0.4$
$\beta = 0.3$	No Surrender Provision	No Mortality Risk		61	130	198
		With Mortality Risk		60	129	196
	With Surrender Provision	No Mortality Risk		61	205	476
		With Mortality Risk		60	196	460
$\beta = 0.5$	No Surrender Provision	No Mortality Risk		61	132	202
		With Mortality Risk		60	130	200
	With Surrender Provision	No Mortality Risk		61	206	478
		With Mortality Risk		60	198	461
$\beta = 0.7$	No Surrender Provision	No Mortality Risk		60	133	207
		With Mortality Risk		59	131	204
	With Surrender Provision	No Mortality Risk		61	211	487
		With Mortality Risk		60	202	469
		$T = 25$	$G = 4$	$\sigma = 0.2$	$\sigma = 0.3$	$\sigma = 0.4$
$\beta = 0.3$	No Surrender Provision	No Mortality Risk		42	94	146
		With Mortality Risk		41	93	144
	With Surrender Provision	No Mortality Risk		42	151	380
		With Mortality Risk		41	142	362
$\beta = 0.5$	No Surrender Provision	No Mortality Risk		41	95	147
		With Mortality Risk		40	93	145
	With Surrender Provision	No Mortality Risk		42	151	378
		With Mortality Risk		40	142	359
$\beta = 0.7$	No Surrender Provision	No Mortality Risk		40	92	145
		With Mortality Risk		39	92	146
	With Surrender Provision	No Mortality Risk		41	154	382
		With Mortality Risk		40	144	362

Table 9: Fair fees (in bp) of GMWBs under the CEV model computed using the willow tree method.

Parameter values are $m = 100$, $r = 3.25\%$ and $\eta = 10\%$.

$T = 20$	r	0.03	0.04	0.05
	Static	69	37	16
$\beta = 0.3$	Mix	113	43	18
	Dynamic	165	77	26
	Static	69	37	16
$\beta = 0.5$	Mix	112	42	16
	Dynamic	162	74	25
	Static	69	37	15
$\beta = 0.7$	Mix	110	42	15
	Dynamic	159	73	23
$r = 5\%$	T	20	25	30
	Static	69	49	36
$\beta = 0.3$	Mix	113	81	60
	Dynamic	165	123	92
	Static	69	48	35
$\beta = 0.5$	Mix	112	80	58
	Dynamic	162	119	88
	Static	69	48	34
$\beta = 0.7$	Mix	110	79	56
	Dynamic	159	117	86

Table 10: Fair fees (in bp) of GMWBs under the CEV model computed using the willow tree method under static, mix and dynamic withdrawals. The underlying fund volatility is $\sigma = 0.2$ and penalty is $\eta = 5\%$.

	Fee (bp)
Huang <i>et al.</i> (2012)	454.52
WTM	453.44

Table 11: Fair fees (in bp) of GMWB under Merton's jump-diffusion model computed using the WTM and the method in Huang *et al.* (2012) with dynamic withdrawals. The parameter values are $T = 10$, $r = 5\%$, $\sigma = 0.3$, $\alpha_J = -0.9$, $\sigma_J = 0.45$, $\lambda = 0.1$ and penalty $\eta = 10\%$.

	$T = 20$	r (%)	3	4	5	6	7
Static	WTM	Fee (bp)	68	41	25	16	10
	BMM	Fee (bp)	66	41	25	16	10
Mix	WTM	Fee (bp)	87	42	25	16	10
	BMM	Fee (bp)	83	40	25	16	10
Dynamic	WTM	Fee (bp)	138	69	37	23	15
	BMM(bang-bang)	Fee (bp)	88	44	29	19	15
	BMM(brute search)	Fee (bp)	469	129	46	27	16
	$r = 5\%$	T	10	15	20	25	30
Static	WTM	Fee (bp)	84	44	25	16	11
	BMM	Fee (bp)	82	43	25	16	12
Mix	WTM	Fee (bp)	84	44	25	16	11
	BMM	Fee (bp)	82	43	25	16	12
Dynamic	WTM	Fee (bp)	99	61	37	23	15
	BMM(bang-bang)	Fee (bp)	88	46	29	22	18
	BMM(brute search)	Fee (bp)	201	95	46	28	18

Table 12: Fair fees (in bp) of GMWB under Merton’s jump-diffusion model computed using the WTM and BMM method with static, mix and dynamic approaches where the parameters for the jump-diffusion model are $\sigma = 0.1114$, $\alpha_J = -0.1825$, $\sigma_J = 0.1094$, $\lambda = 0.5282$ and penalty $\eta = 5\%$.

$T = 20$	$r = 5\%$	η (%)	0	1	2	3	4	5
Static	WTM	Fee (bp)	25	25	25	25	25	25
	BMM	Fee (bp)	25	25	25	25	25	25
Mix	WTM	Fee (bp)	97	58	36	26	25	25
	BMM	Fee (bp)	94	55	34	25	25	25
Dynamic	WTM	Fee (bp)	234	167	111	71	45	37
	BMM(bang-bang)	Fee (bp)	96	58	37	29	29	29
	BMM(brute search)	Fee (bp)	195	142	103	75	57	46

Table 13: Sensitivity of fair fees (in bp) with respect to the penalty charge η computed using the willow tree method (WTM) and BMM method under Merton’s jump-diffusion model. Parameter values are $\sigma = 0.1114$, $\alpha_J = -0.1825$, $\sigma_J = 0.1094$, and $\lambda = 0.5282$.

Panel A: Typical specification of the time-dependent penalty charge η ,
 which decreases as the calendar time progresses.

Year	$0 \leq t \leq 5$	$5 < t \leq 10$	$10 < t \leq 15$	$15 < t \leq 20$
η (%)	3.0	2.5	2.0	1.5

Panel B: Computed fair fees for GMWB.

	Static	Mix	Dynamic
Fee (bp)	25	28	73

Table 14: The fair fees (in bp) for a 20-year GMWB are computed based on the given decreasing time-dependent penalty charge (see Panel A) under the static, mix and dynamic withdrawals. The underlying fund dynamics follows Merton's jump-diffusion process with $r = 5\%$, $\sigma = 0.1114$, $\alpha_J = -0.1825$, $\sigma_J = 0.1094$ and $\lambda = 0.5282$.